Fucoidan-functionalized polysaccharide submicroparticles loaded with alteplase for efficient targeted thrombolytic therapy

Alina Zenych, Charlène Jacqmarcq, Rachida Aid, Louise Fournier, Laura M Forero Ramirez, Thomas Bonnard, Denis Vivien, Didier Letourneur, Cedric Chauvierre

Biomaterials

Fucoidan-Functionalized Polysaccharide Submicroparticles Loaded with Alteplase for Efficient Targeted Thrombolytic Therapy

--Manuscript Draft--

Manuscript Number:	
Article Type:	FLA Original Research
Keywords:	nanomedicine; drug delivery; targeted thrombolysis; polysaccharides; fucoidan; P-selectin
Corresponding Author:	Cedric CHAUVIERRE, Dr INSERM U1148: Laboratoire de Recherche Vasculaire Translationnelle Paris, FRANCE
First Author:	Alina Zenych, Dr
Order of Authors:	Alina Zenych, Dr
	Charlène Jacqmarcq
	Rachida Aid
	Louise Fournier
	Laura M. Forero Ramirez, Dr
	Thomas Bonnard, Dr
	Denis Vivien, Pr
	Didier Letourneur, Dr
	Cedric CHAUVIERRE, Dr
Abstract:	Intravenous administration of fibrinolytic drugs is the standard treatment of acute thrombotic diseases. However, current fibrinolytics exhibit limited clinical efficacy because of their short plasma half-lives and might trigger hemorrhagic transformations. Therefore, it is mandatory to develop innovative nanomedicine-based solutions for more efficient and safer thrombolysis with biocompatible and biodegradable thrombus-targeted nanocarrier. Herein, fucoidan-functionalized hydrogel polysaccharide submicroparticles with high biocompatibility are elaborated by the inverse miniemulsion / crosslinking method. They are loaded with the gold standard fibrinolytic – alteplase – to direct site-specific fibrinolysis due to nanomolar interactions between fucoidan and P-selectin overexpressed on activated platelets and endothelial cells in the thrombus area. The thrombus targeting properties of these particles are validated in a microfluidic assay containing recombinant P-selectin and activated platelets under arterial and venous blood shear rates as well as in vivo. The experiments on the murine model of acute thromboembolic ischemic stroke support this product's therapeutic efficacy, revealing a faster recanalization rate in the middle cerebral artery than with free alteplase, which reduces post-ischemic cerebral infarct lesions and blood-brain barrier permeability. Altogether, this proof-of-concept study demonstrates the potential of a biomaterial-based targeted nanomedicine for the precise treatment of acute thrombotic events, such as ischemic stroke.

LVTS UMRS 1148
Laboratory for Vascular Translational Science
Université de Paris
Inserm
La science pour la santé
From science to health
UNIVERSITÉ PARIS 13

Paris, February 9, 2021

Dear Editor,

Please find enclosed the manuscript entitled "**Fucoidan-functionalized polysaccharide submicroparticles loaded with alteplase for efficient targeted thrombolytic therapy**" to be considered for publication in Biomaterials.

Ischemic stroke, myocardial infarction and venous thromboembolism are the main causes of death worldwide. Treatment of acute thrombotic events remains a challenge. Indeed, less than 5% of patients are injected with the standard thrombolytic drug, because of serious side effects associated with the treatment. It is thus important to create innovative nanomedicine-based solutions for more efficient and safer thrombolysis with biocompatible and biodegradable thrombus-targeted nanocarrier. In this work, polysaccharide biocompatible submicroparticles were elaborated by an original green chemistry method with all materials approved for use in humans. They were functionalized with a fucoidan that has a nanomolar affinity for the thrombus biomarker P-selectin and already used in clinical trials for molecular imaging of thrombotic diseases. Alteplase was loaded onto these hydrogel submicroparticles, the thrombolytic efficacy of the nanomedicine-based product was successfully validated in a murine model of acute ischemic stroke. This is a proof-of-concept study of the high potential of a biomaterial-based targeted nanomedicine for the precise treatment of acute thrombotic events, such as ischemic stroke.

We believe that this research article focused on the hot topics of nanomedical approaches with a translational potential for a major health issue would be of interest to the interdisciplinary audience of your highly ranked journal.

All co-authors agree with the contents of the manuscript and there is no financial interest to report. We certify that the submission is an original unpublished work and it has not been submitted to any other journal for review.

Hoping that you will find this work of interest, we are looking forward to hearing from you.

Yours sincerely,

Dr. Cédric Chauvierre
Inserm, U1148, LVTS, Université Paris, CHU X. Bichat, F-75877, Paris, France
E-mail address: cedric.chauvierre@inserm.fr
Tel: (33) 1 4025 8600; Fax: (33) 1 4025 8602

Fucoidan-Functionalized Polysaccharide Submicroparticles Loaded with Alteplase for Efficient Targeted Thrombolytic Therapy

Alina Zenych[1], Charlène Jacqmarcq[2,#], Rachida Aid[1,3,#], Louise Fournier[1], Laura M. Forero Ramirez[1], Thomas Bonnard[2], Denis Vivien[2,4,#], Didier Letourneur[1,#], and Cédric Chauvierre[1,*]

[1] Université de Paris, Université Sorbonne Paris Nord, UMR S1148, INSERM, F-75018 Paris, France
[2] INSERM U1237 Physiopathology and Imaging of Neurological Disorders (PhIND), Institut Blood and Brain @ Caen Normandie (BB@C), GIP Cyceron, 14074, Caen, France
[3] Université de Paris, FRIM, UMS 034, INSERM, F-75018 Paris, France
[4] Department of Clinical Research, Caen Normandie University Hospital (CHU), 14074 Caen, France.

[*] Corresponding author: Université de Paris, Université Sorbonne Paris Nord, UMR S1148, INSERM, F-75018 Paris, France
E-mail address: cedric.chauvierre@inserm.fr
[#] Equal contribution

Fucoidan-Functionalized Polysaccharide Submicroparticles Loaded with Alteplase for Efficient Targeted Thrombolytic Therapy

Alina Zenych[1], Charlène Jacqmarcq[2,#], Rachida Aid[1,3,#], Louise Fournier[1], Laura M. Forero Ramirez[1], Thomas Bonnard[2], Denis Vivien[2,4,#], Didier Letourneur[1,#], and Cédric Chauvierre[1,*]

[1] Université de Paris, Université Sorbonne Paris Nord, UMR S1148, INSERM, F-75018 Paris, France
[2] INSERM U1237 Physiopathology and Imaging of Neurological Disorders (PhIND), Institut Blood and Brain @ Caen Normandie (BB@C), GIP Cyceron, 14074, Caen, France
[3] Université de Paris, FRIM, UMS 034, INSERM, F-75018 Paris, France
[4] Department of Clinical Research, Caen Normandie University Hospital (CHU), 14074 Caen, France.

[*] Corresponding author: Université de Paris, Université Sorbonne Paris Nord, UMR S1148, INSERM, F-75018 Paris, France
E-mail address: cedric.chauvierre@inserm.fr
[#] Equal contribution

ABSTRACT

Intravenous administration of fibrinolytic drugs is the standard treatment of acute thrombotic diseases. However, current fibrinolytics exhibit limited clinical efficacy because of their short plasma half-lives and might trigger hemorrhagic transformations. Therefore, it is mandatory to develop innovative nanomedicine-based solutions for more efficient and safer thrombolysis with biocompatible and biodegradable thrombus-targeted nanocarrier. Herein, fucoidan-functionalized hydrogel polysaccharide submicroparticles with high biocompatibility are elaborated by the inverse miniemulsion / crosslinking method. They are loaded with the gold standard fibrinolytic – alteplase – to direct site-specific fibrinolysis due to nanomolar interactions between fucoidan and P-selectin overexpressed on activated platelets and endothelial cells in the thrombus area. The thrombus targeting properties of these particles are validated in a microfluidic assay containing recombinant P-selectin and activated platelets under arterial and venous blood shear rates as well as *in vivo*. The experiments on the murine model of acute thromboembolic ischemic stroke support this product's therapeutic efficacy, revealing a faster recanalization rate in the middle cerebral artery than with free alteplase, which reduces post-ischemic cerebral infarct lesions and blood-brain barrier permeability. Altogether, this proof-of-concept study demonstrates the potential of a biomaterial-based targeted nanomedicine for the precise treatment of acute thrombotic events, such as ischemic stroke.

Keywords: nanomedicine, drug delivery, targeted thrombolysis, polysaccharides, fucoidan, P-selectin

1. INTRODUCTION

Acute thrombotic pathologies such as myocardial infarction, ischemic stroke, and venous thromboembolism remain a major global healthcare challenge contributing to a significant number of deaths and disabilities.[1] Current thrombolytic therapy, the intravenous injection of Plasminogen Activators (PA), is administrated to lyse a clot-induced vascular occlusion and restore the blood flow in the vessel. The recombinant tissue plasminogen activator (rtPA) is the most commonly applied clot-busting drug in clinics and the only one approved to treat acute ischemic stroke.[2] rtPA is a fibrin-specific serine protease that activates the endogenous proenzyme plasminogen and converts it to the active form plasmin, thus, degrading the thrombus fibrin network. However, systemic delivery of rtPA is limited by the rapid drug elimination (half-life 4-6 min), physiological deactivation by its antidotes such as Plasminogen Activator Inhibitors (PAI-1 and PAI-2), and deleterious side-effects such as intracranial hemorrhages.[3] This restricts its use to a narrow therapeutic window (4.5 h of stroke symptom onset when injected alone and 6 h when combined with mechanical thrombectomy) beyond which the deleterious effects of rtPA overcome its benefits. Moreover, the rate of acute recanalization after intravenous administration of rtPA is low: only ~30% of patients experienced full or partial recanalization.[4]

Therapeutic strategies that intend to address the challenges of thrombolytic therapy and boost survival rates remain of great clinical interest. Certainly, novel thrombolytic molecules are being researched to increase reperfusion, improve safety, and protect the brain neurovascular unit.[5,6] Apart from that, nanomedical approaches for the targeted delivery of thrombolytic agents have been intensively proposed.[7] Korin *et al.* reported the microaggregates of poly (lactic-co-glycolic acid) (PLGA) nanoparticles (NPs) dissociated into rtPA-bearing nanocompounds when exposed to abnormally high hemodynamic shear stress, typical for the vascular occlusions, that performed effective thrombolysis in several preclinical

models.[8] Colasuonno *et al.* formulated rtPA-loaded discoidal porous nanoconstructs from a mixture of PLGA and polyethylene glycol (PEG) with high thrombolytic potential presumably attributed to the erythrocyte-mimicking shape of the NPs and their deformability, leading to efficient circulation profiles and accumulation on the clot.[9] While these nanosystems with passive targeting succeeded in a promising thrombolytic efficacy in preclinical studies, more recent and advanced examples are formulated with actively targeted nanocarriers.

Active targeting permits drug accumulation specifically at the thrombus site and has the potential to enhance the enzyme penetration into deeply localized thrombi. Apart from the magnetic nanoparticle targeting under an external magnetic field, active blood clot targeting is currently achieved by directing the functionalized NPs towards fibrin or activated platelets (mostly integrin GPIIb/IIIa and less adhesion receptor P-selectin) with antibodies and/or peptides. Notably, a theranostic system for thrombus molecular imaging and targeted therapy was developed by Zhou *et al.* when rtPA was encapsulated into the Fe_3O_4-based PLGA NPs, and a cyclic arginine-glycine-aspartic acid (cRGD) peptide was grafted onto the chitosan surface to target GPIIb/IIIa on activated platelets.[10] Nevertheless, both antibodies and peptides have their limitations for targeted drug delivery. The immunogenicity, purity, and sufficient circulation time are the main concerns of the application of the antibodies[11], while peptides might suffer from weak binding affinity, immunogenicity, a high costs of peptide synthesis, and metabolic instability with fast renal clearance due to their small sizes.[12]

An effective alternative could be the nanoparticle functionalization with fucoidan,[13] a naturally-occurring algae-derived sulfated polysaccharide that exhibits a strong and specific tropism for the P-selectin overexpression in cardiovascular pathologies.[14,15] Fucoidan emerged as an affordable, high-quality targeting ligand to P-selectin that was prior validated by our group on various polysaccharide-based nano- & microsystems for molecular diagnostics and targeted therapy.[16–20] Following the obtention of the label “raw materials for

pharmaceutical uses" in 2015 in France, it became a part of the large-scale European Union project NanoAthero as a contrast agent for Single-Photon Emission Computed Tomography (SPECT) imaging in human atherothrombosis, coordinated by our laboratory.[21] The first in the world Phase I clinical trial on intravenous delivery of fucoidan radiolabeled by Technetium-99m reported its safety and favorable biodistribution,[22] while Phase IIa for the imaging of deep vein thrombosis and pulmonary embolism is ongoing.

It is critical to ensure an excellent safety profile of the designed nanocarrier for targeted thrombolysis in future clinical translation by selecting biocompatible and fully biodegradable materials with the U.S. Food and Drug Administration (FDA)-approval.[23] Contrary to the attractiveness of synthetic polymers such as PLGA, the NPs made of polysaccharides are explored to a lesser degree for thrombolytic therapy. Yet, they benefit from the general advantages of natural polymers: biocompatibility, low cost, and hydrophilicity. Polysaccharide hydrogels, which are crosslinked three-dimensional polymer networks, absorb large quantities of water and can effectively load macromolecules with high encapsulation efficiency,[24] including plasminogen activators. Few publications reported the nanoformulations with chitosan, a cationic chitin-derived polysaccharide that can form polyelectrolyte complexes with negatively charged molecules.[25] For instance, superior thrombolytic potential *in vivo* was demonstrated on self-assembled chitosan NPs crosslinked with sodium tripolyphosphate and loaded with urokinase.[26] Liao *et al.* formulated the lumbrokinase-bearing NPs from quaternized derivative of chitosan - N,N,N-Trimethyl Chitosan covalently grafted with cRGD peptide to target GPIIb/IIIa receptors that could accelerate thrombolysis.[27]

Dextran, an exocellular bacterial water-soluble polysaccharide, is extensively employed in clinics, particularly in its low molecular weight (40 and 70 kDa), for plasma volume expansion, thrombosis prophylaxis, peripheral blood flow enhancement, artificial tears, *etc*. [28] Dextran coating of magnetic NPs is applied to ensure their environmental stability and prolong

the blood circulation time.[29,30] However, there is no reported exclusively dextran nanocarrier with hydrogel structure for thrombolytic application to our knowledge. Meeting the requirements of biocompatibility, biodegradability, non-immunogenicity, dextran stands out as an attractive polymer to design an alteplase delivery system.

Herein, we fabricated novel fucoidan-functionalized dextran submicroparticles (SPs) by a green chemistry method using fully biodegradable and biocompatible compounds, all of them approved by the FDA. After physico-chemical and biosafety characterization of these hydrogel-like SPs, rtPA was loaded onto the SPs with a high encapsulation capacity, and its release in saline and *in vitro* amidolytic and fibrinolytic activities were tested. Through the *in vitro* microfluidic experiments under continuous arterial or venous flow, we provided evidence that fucoidan-functionalized SPs (Fuco-SPs) have a high and specific affinity to P-selectin and accumulate on activated platelet aggregates. Also, these particles bind to the thrombi *in vivo*. Finally, rtPA-associated Fuco-SPs proved superior *in vivo* thrombolytic efficacy in a mouse stroke thrombin model with a faster vessel recanalization that minimized cerebral tissue damage: the post-ischemic lesion and blood-brain barrier (BBB) permeability.

2. MATERIALS AND METHODS

Materials: Dextran 40 kDa and TRITC-dextran 40 kDa were provided by TdB Consultancy (Uppsala, Sweden). Fucoidan (Mn = 18 kDa/Mw = 104 kDa) was a gift from Algues & Mer (Ouessant, France). Sodium trimetaphosphate (STMP), methylene blue hydrate, and Human Serum Albumin (HSA) were purchased from Sigma-Aldrich (Saint-Quentin-Fallavier, France). Polyglycerol polyricinoleate (PGPR) was obtained from Palsgaard France S.A.S. (Lyon, France). Vegetable (sunflower) oil was purchased from a local supermarket. The SPs were encapsulated with commercially available rtPA (Actilyse®, Boehringer Ingelheim) that was reconstituted at 1 mg/ml, aliquoted, and stored at -80 ° C. Chromatography paper was

obtained from GE Healthcare (Chicago, Illinois, United States). Fibrillar type I collagen Horm® was obtained from Takeda (Linz, Austria). 96-Well Cell Culture Plates (Costar) were obtained from Corning Incorporated. PPACK (Phe-Pro-Arg-Chloromethylketone) 75 µM tubes were purchased from Cryopep (Montpellier, France). Flow chambers (Vena8 Fluoro+) were provided from Cellix Ltd (Dublin, Ireland).

Submicroparticle synthesis: Polysaccharide submicroparticles (SPs) were obtained via a water-in-oil (w/o) emulsification combined with a crosslinking process.[16,17] Polysaccharide solution (300 mg/ml, 6 M NaCl) was prepared as a mixture of dextran 40 and 5% TRITC-dextran 40 (for fluorescent SPs). To synthesize functionalized SPs with fucoidan (Fuco-SPs), 10% w/w of fucoidan was added. **Table** S1, Supplementary Data describes the synthesis parameters of SPs.

First, the organic phase of 15 mL of sunflower oil and 6% w/v PGPR in Falcon® 50 mL was prepared and cooled down for 20 min at -20 ° C. In the meantime, 1,200 mg of the polysaccharide solution was incubated with 120 µL of 10 M NaOH under magnetic stirring for 10 min. 240 µL of STMP solution (30% w/v in water) was added into the aqueous phase under magnetic stirring and mixed for 20 seconds on ice. Next, emulsification was achieved by the dropwise injection of 600 µL of the aqueous phase into the organic phase and dispersed with a stand-disperser (Polytron PT 3100, dispersing aggregate PT-DA 07/2EC-B101, Kinematica, Luzernerstrasse, Switzerland) at 30,000 rpm for 4 min on ice. The obtained w/o emulsion was transferred into 50 ° C for the crosslinking reaction of polysaccharides with STMP for 20 min. The crosslinked suspension was washed in 30 mL PBS 10x for 40 min under high magnetic stirring at 750 rpm. The mixture was then centrifuged (BR4i, JOUAN SA, Saint Herblain, France) for 10 min at 3,000 g in Falcon tubes. The organic phase was recovered and ultracentrifuged (Optima MAX-XP, Ultracentrifuge, Beckman Coulter, Brea, California, United States) in PBS for 45 min at 15,000 g. The obtained pellet was washed by

ultracentrifugation 2 times in 0.04% Sodium Dodecyl Sulfate (SDS) solution and then 3 times in ultrapure water to purify the SPs. The resulting SPs were suspended in water or 0.9% NaCl with 0.02% Tween 20 (Sigma) and stored at 4 ° C.

Cell culture and cytotoxicity assay: To evaluate the cytotoxicity of the SPs, Fluorometric Cell Viability Assay (Resazurin) was used on confluent Human Umbilical Vein Endothelial Cells (HUVECs). The cells were cultured in DMEM supplemented with 10% (v/v) fetal bovine serum, 4 mmol of l-glutamine, 100 units/ml of penicillin, and 100 µg/ml of streptomycin and kept in an incubator at 37 °C in a humidified atmosphere of 5% CO_2. Cells were seeded into 96-well plates to adhere, 10,000 cells per well. Following 24 h of incubation to reach ~80% confluency, the medium in the wells was changed to the one containing the SPs at concentrations ranging from 0.1 to 1.5 mg/ml and cultured for another 24h. The SPs were prior sterilized under the UV light for 15 min. Next, the medium was replaced with 100 µL 10% Resazurin solution, and the plates were covered in foil and incubated for 2h. Culture media were used as a positive control. The Resazurin's fluorescent signals were monitored using 540 nm excitation and 590 nm emission wavelengths on Infinite® 200 PRO microplate reader (TECAN Group Ltd., Mannedorf, Switzerland). The obtained fluorescence (Fl) values were blank corrected, and the relative cell viability was expressed as Fl_{SPs} / $Fl_{control}$ × 100%, where $Fl_{control}$ was obtained in the absence of the SPs. The experiment was performed in hexaplicate.

To examine the potential cell cytoskeleton organization mediated by Fuco-SPs, HUVECs cells were cultured in 8-well Lab-Tek II Chamber Slide w/Cover (Lab-Tek®, Thermo Fischer Scientific, Massachusetts, United States) with 10,000 cells per well. The wells' medium was changed 24 h after to the one containing TRITC-Fuco-SPs at 1.5 mg/ml and was incubated for another 24 h. Cells cultured in the medium without the SPs were set as control. Next, cells were fixed with 4% paraformaldehyde for 30 min at room temperature (RT). After rinsing with PBS, cells were labeled and permeabilized with the 200 µl mixture of FITC-Phalloidin (1:200,

Sigma-Aldrich, USA) / DAPI (1:100, Thermo Fisher Scientific, Massachusetts, United States) / 0.01% v/v Tween 20 in PBS and incubated under low agitation for 1 h at RT. The cells were afterward washed 3 times with PBS. The support of the chamber slides was removed, and the slides were mounted with a few drops of the aqueous mounting medium and kept at 4° C until visualization with the confocal microscope (Zeiss LSM 780, Iena, Germany).

Hemocompatibility test: Hemolysis assay was adapted from the publication[17] and performed on washed isolated murine erythrocytes. Murine blood was collected in sodium citrate 3.8% (w/v) and centrifuged at 800 g for 5 min to isolate red blood cells. The supernatant was removed, and the pellet of erythrocytes was resuspended at 20% (v/v) in distilled water (positive control, 100% hemolysis), normal saline (negative control, no hemolysis), and the Fuco-SPs at concentrations from 0.1 to 1.5 mg/ml in Eppendorf. The tubes were incubated on a rotator at 37 °C for 1.5 h and then centrifuged at 3,000 g for 5 min. The absorbance (A) of the supernatants was measured on Infinite® 200 PRO microplate reader (TECAN Group Ltd., Mannedorf, Switzerland) at 590 nm. Each sample was run in triplicate. The percentage of hemolysis was determined by the formula: Hemolysis degree (%) = 100% x $(A_{sample} - A_{negative\ control})/(A_{positive\ control} - A_{negative\ control})$.

Physico-chemical characterization: The submicroparticle (SP) formulations were studied for particle morphology, size and zeta potential distributions, mass concentration, and elemental composition.

Particle morphology was visualized by Transmission Electron Microscopy (TEM) (Philips FEI Tecnai 12, Amsterdam, Netherlands), negatively stained with 1% (w/v) uranyl acetate for 5 minutes, and Environmental Scanning Electron Microscopy (ESEM) (Philips XL30 ESEM-FEG, Amsterdam, Netherlands). Hydrodynamic size and Zeta potential (ζ-potential) were measured by Dynamic Light Scattering (DLS) and Electrophoretic Light Scattering (ELS), respectively (Zetasizer Nano ZS, Malvern Instruments SARL, Orsay,

France). Samples were diluted in distilled water or saline for size and in 1 mM KCl for ζ-potential determination. All runs were performed at 25 °C in triplicate.

Mass concentration was determined by freeze-drying. An elemental analyzer-mass spectrophotometer was used for the quantification of the sulfur (presence of fucoidan). To prove the crosslinking with STMP, the total reflection X-ray fluorescence spectroscopy (TXRF) technique was applied to quantify the phosphorus content on the SPs (S2 PICOFOX Bruker, Massachusetts, United States).

Sulfate and fucoidan quantification: The sulfate content of fucoidan was determined by a semi-quantitative solid-phase colorimetric assay.[72] Briefly, 5 µL of Fuco-SPs in suspension at a concentration of 2 mg/ml were dropped on a piece of Whatman Chromatography paper grade 1. This was repeated 5 times on the same point, allowing the paper to dry at 50 ° C in between. The paper was first soaked into a methanol/acetone (6:4) solution for 3 min and then into a methanol/acetone/water (6:4:15) solution with 50 mM HCl and 0.1% w/w methylene blue for 10 min. Finally, the paper was extensively washed with acetic acid/methanol/acetone/water (5:6:4:75) until no coloration was detected in the washing solution. The paper was then transferred to the Eppendorf, containing 0.5 mL methanol with 2% w/v SDS, and incubated for 15 min at 50 ° C. 0.2 mL of the extracted dye was placed in a 96-well plate, and its concentration was determined by reading absorbance at 663 nm on an Infinite® 200 PRO microplate reader (TECAN Group Ltd., Mannedorf, Switzerland). Standard curves were obtained from fucoidan in solution with known concentrations.

Loading rtPA on the SPs: rtPA was immobilized onto the SPs by adsorption. 100 µl of SPs (5 mg/ml) was mixed with 100 µl of rtPA (1 mg/ml) in ultrapure water and then incubated for 1 h at RT. Free unabsorbed rtPA was removed by 3 cycles of ultracentrifugation (15 min, 15,000 g). The SPs with adsorbed rtPA (rtPA-SPs) were resuspended in water and used for the drug loading efficiency quantification.

Drug encapsulation efficiency: The amount of rtPA loaded on the SPs was measured using the Pierce BCA protein assay kit (Life Technologies SAS, Courtaboeuf, France). Briefly, 200 µl of working reagent was added to 25 µL of each sample in 96 well-plate. The absorbance at 562 nm was read on the Infinite® 200 PRO microplate reader (TECAN Group Ltd., Mannedorf, Switzerland) after 30 min of incubation at 37 °C and cooling to RT for 10 min. The concentration of the drug was extrapolated by a calibration curve prepared with different concentrations of rtPA.

The encapsulation efficacy (EE) was calculated as EE (%) = 100% x B/A, whereas B is the amount of rtPA loaded onto the SPs and A is the total quantity of rtPA put in contact with the SPs.

In vitro rtPA release: The release of rtPA from the Fuco-SPs was assessed by flow cytometry.[44] FITC-rtPA (Abcam, Cambridge, United Kingdom) at 1 mg/ml was placed in contact with TRITC Fuco-SPs at 5 mg/ml for 1 h at RT. The suspensions were added to tubes pre-filled with 400 µL of saline and placed under gentle agitation at 37 ° C. At each time point of 0, 15, 30, 45, 60, and 90 min, the tubes were analyzed with a BD FACS Aria™ III flow cytometer (Becton Dickinson, New Jersey, United States). The TRITC-Dextran, excited by a 543 nm laser, was detected at 569 nm, while the FITC-rtPA, excited at 480 nm, was detected on a 530/30 nm PMT. Flow cytometry analyses were performed in triplicates with Diva software (Becton Dickinson). The protein release curve was obtained by normalizing the values of Mean Fluorescence Intensity (MFI) of the FITC-rtPA still associated with TRITC-Fuco-SPs.

In vitro amidolytic activity of rtPA-loaded SPs: Amidolytic activity of rtPA loaded SPs was assessed with the fluorogenic substrate PefaFluor® tPA (Cryopep, Montpellier, France). 2.5 µL of samples (20 µg/ml) was put in contact with 97.5 µL of 100 mM HEPES buffer (pH 8.0, 154 mM NaCl, 0.1% HAS) in the 96-well plate. After the addition of 10 µL PefaFluor® at 1 mM, a kinetic profile was obtained by measuring the fluorescence level at 440 nm every 2

min for 90 min at 37 ° C with Infinite® 200 PRO microplate reader (TECAN Group Ltd., Mannedorf, Switzerland). Free rtPA was used at the same concentration based on the Pierce BCA protein assay. Increase of fluorescence corresponded to the fluorogenic peptide substrate hydrolysis by rtPA. Enzymatic activity was determined from the resulting kinetic profile and compared to the one of free rtPA.

In vitro fibrinolytic activity of rtPA-loaded SPs: To assess the fibrinolytic activity of rtPA-loaded SPs, a fibrin lysis clot experiment was performed. 5 mL of TRIS Buffer with 3% w/v low melting agarose (Carl Roth GmbH þ Co. KG, Karlsruhe, Germany) were heated to 65 °C. 5 mL of fibrinogen (from human plasma, Sigma Aldrich) solution in TRIS buffer (5 mg/ml) was slowly heated to 37 °C. Once the agarose solution reached 65 °C, it was cooled to 37 °C, and 2.5 U of thrombin (from human plasma, Sigma Aldrich) was added. Next, a fibrinogen solution was slowly added into the agarose/thrombin mixture under gentle agitation to avoid the formation of bubbles. The reaction mixture was poured into a 9 cm Petri dish and cooled at 4 °C for 30 min until the fibrin clot became visible. On the solidified agarose gel, round wells were formed using a 3 mm punch as sample reservoirs. 5 µL of each SPs sample (45 µg/ml) was dropped into the wells and incubated overnight at 37 °C in a humid environment. The degree of fibrin lysis was quantified with ImageJ by comparing the size of the fibrinolysis circle of the samples and free rtPA at the equivalent concentration based on the Pierce BCA protein assay.

Flow microchamber experiments: An *in vitro* flow adhesion assay was performed to evaluate the affinity of the Fuco-SPs with their molecular target. Micro-channels of Vena8 Fluoro^{+} chambers (width: 0.04 cm, height: 0.01 cm, and length: 2.8 cm; Cellix Ltd, Dublin, Ireland) were coated overnight with recombinant human P-selectin, L-selectin or E-selectin (R&D systems France, Lille, France) at 100 µg/ml and left overnight at 4 °C. To confirm the concentration-dependent binding of Fuco-SPs to P-selectin, some channels were coated with P-

selectin at a range of concentrations (5, 25, 50, and 100 µg/ml). Channels were then washed with NaCl 0.9% and further incubated with HSA at 10 µg/ml for 2 h.

A suspension of fluorescently labeled Control-SPs or Fuco-SPs (1 mg/ml) in saline was passed through the channels for 5 min at arterial and venous flow conditions (shear stress 67.5 dyne/cm^2 and 6.75 dyne/cm^2) using an ExiGo™ pump (Cellix Ltd, Dublin, Ireland). For the competitive binding experiment, fucoidan solution (10 mg/ml) was injected 5 min prior to the Fuco-SPs at the same rate. Then, all the channels were washed with NaCl 0.9% for 1 min. The binding of the adhered SPs was visualized in real-time under fluorescence microscopy (Axio Observer, Carl Zeiss Microimaging GmbH, Iena, Germany). For the quantitative analysis, the number of fluorescent SP clusters on each channel was measured using the "Analyze particles" tool in the image analysis software ImageJ (NIH, Bethesda, U.S.) with a 4-pixel threshold to eliminate the background noise.

To further investigate the binding efficiency of unloaded and loaded SPs to activated platelets, the microchannels of Vena8 Fluoro$^+$ were coated with fibrillar type I collagen Horm® (50 µg/ml) overnight at 4 °C and rinsed with NaCl 0.9% before use. Human whole blood (EFS, Bichat Hospital, Paris, France), collected in the PPACK tubes and labeled with 5 µM DIOC6 (Life Technologies SAS, Saint-Aubin, France), was perfused at arterial shear stress for 5 min to induce platelet activation and aggregation. Platelet aggregation through contact with collagen was visualized in real-time with phase-contrast microscopy (Axio Observer, Carl Zeiss Microscopy, Oberkochen, Germany). After rinsing with NaCl 0.9%, fluorescent Control-SPs or Fuco-SPs (unloaded or loaded with rtPA) at 1 mg/ml were injected into the channels in saline for 5 min. Their accumulation onto activated aggregates was monitored in real-time. Channels were then washed for 1 min with NaCl 0.9%. Finally, the MFI of the fluorescent SPs bound to the platelets on each channel was analyzed with ImageJ. Intensity settings were kept the same for both types of SPs.

Tissue distribution of Fuco-SPs in vivo: Animal studies were performed on C57BL/6 male mice (EJ, Le Genest, St-Berthevin, France) aged 5-8 weeks (~ 25 g weight) in respect of the principles of laboratory about animal experimentation and with the approval of the animal care and use committee of the Claude Bernard Institute (APAFIS #8724, Paris, France). Mice were anesthetized under the application of 2% isoflurane (Aerrane, Baxter). 200 µL of Fuco-SPs (5 mg/ml) were injected through the retro-orbital route (n=3). To histologically analyze the particle accumulation, mice were sacrificed 30 min following their administration. The liver, spleen, lungs, and kidneys were excised, washed in saline, and fixed in paraformaldehyde 4%. The tissues were then frozen and cryosectioned at 10 µm thickness. The samples were stained with alcian blue & nuclear fast red staining protocol. Strongly negative structures, including the Fuco-SPs, are stained blue, nuclei are stained pink to red, and cytoplasms appear pale pink. The slides with tissue slices were scanned with the Nanozoomer (Hamamatsu, Hamamatsu City, Japan) and viewed with the NDP.view2 software.

Animals and thromboembolic stroke model in vivo: Animal experiments were carried out on male Swiss wild-type mice (8–9 weeks old; 35-45 g; CURB, Caen, France). All experiments were performed following the French (Decree 87/848) and the European Communities Council (2010/63/EU) guidelines and were approved by the institutional review board (French ministry of Research). All the experiments were validated by the local ethical committee of Normandy (CENOMEXA) registered under the reference number APAFIS#13172. Anesthesia was induced by the application of 5% isoflurane (Aerrane, Baxter) and maintained by 2% isoflurane in a mixture of O_2/N_2O (30% / 70%).

Mice were placed in a stereotaxic device, then a small craniotomy was performed, the dura was excised, and the middle cerebral artery (MCA) was exposed. To induce the occlusion of the MCA, the coagulation cascade was triggered by the pneumatical injection of 1 µL murine α-thrombin (1 IU; Stago BNL) with a glass micropipette, as previously described.[73]

Successful MCA occlusion was confirmed by the Laser Doppler flowmeter (Oxford Optronix). For the treatment, the animals were intravenously injected through a tail vein catheter (200 µL, 10% bolus, 90% infusion over 40 minutes) with either saline, Actilyse® rtPA 10 mg/kg, or rtPA-Fuco-SPs (loaded rtPA at 10 mg/kg, SPs at 71 mg/kg) 20 minutes after thrombus formation (n ≥5). Brain perfusion was monitored by Laser Speckle Contrast Imager (MOOR FLPI-2, Moor Instruments) throughout the treatment. Region of interest (ROI) was selected on the ipsilateral to occlusion and contralateral hemispheres to monitor the relative cerebral blood flow in the affected region Fl_t (%) = 100% x Fl_{ipsi}/Fl_{contra}. The post-stroke reperfusion was expressed as a Growth Rate (GR) of the blood flow increase in the ipsilateral ROI to contralateral one at a time point, and it was quantified as GR (%) = 100% x (Fl_{t2} - Fl_{t1})/ Fl_{t1}.

Magnetic resonance imaging acquisition and analysis: Mice were anesthetized with 5% isoflurane and maintained with 1.5-2% isoflurane in a mixture of O_2/N_2O (30% / 70%) during the acquisitions. Experiments were carried out on a Pharmascan 7T (Bruker Biospin, Wissembourg, France). Three-dimensional T2-weighted images were acquired using a Multi-Slice Multi-Echo sequence (TE/TR 39.9 ms / 3,500 ms, 2 averages) 24 h after the stroke. Lesion volumes were quantified on these images using ImageJ software (slice thickness 0.5 mm). Magnetic resonance angiography was performed using a 2D-TOF sequence (TE/TR 4.24 ms / 12 ms, 1 average) 24 h after ischemia, and the recanalization status of the MCA was determined blindly from the analysis of the merged MCA angiograms with maximum intensity. The angiographic score is based on the TICI (Thrombolysis in Cerebral Infarction) grade flow scoring (from Score 0: no perfusion to Score 3: full recanalization). For the *in vivo* detection of the BBB permeability, three dimensional T1 FLASH sequences (TE/TR 4.37 ms / 15.12 ms; 3 averages) were used, 15 min after the intravenous injection of 200 µL gadolinium chelate (DOTAREM) in saline (0.25 mg/ml). BBB leakage was measured 4 days after the stroke induction, and its volume was quantified using ImageJ.

Thrombus targeting by Fuco-SPs in a murine model of venous thrombosis: Animal studies were done following principles of laboratory animal care and with the approval of the animal care and use committee of the Claude Bernard Institute (APAFIS #8724, Paris, France). $FeCl_3$-induced *in vivo* thrombosis model on mesenteric vein was carried out on C57BL/6 male mice (EJ, Le Genest, St-Berthevin, France) aged 5-8 weeks. Mice were anesthetized with an intraperitoneal injection of ketamine (100 mg/kg) and xylazine (10 mg/kg). After midline abdominal incision, the mesentery was exposed, and vessels were visualized by an intravital microscope (Leica MacroFluo, Leica Microsystems SAS, Nanterre Cedex, France) using Orca Flash 4.0 scientific CMOS camera (Hamamatsu Photonics France SARL, Massy, France). For green fluorescent labeling of mitochondria of platelets and leucocytes, DIOC6 (Life Technologies SAS, Saint-Aubin, France) at 25 µM was retro-orbitally injected. The mesentery vein was covered with a 1 mm Whatman chromatography paper that was prior soaked in a 10% w/v iron chloride (Sigma-Aldrich) solution for 1 min, and then washed with saline. The formation of non-occlusive thrombi was monitored in real-time by fluorescence microscopy by an accumulation of fluorescently labeled platelets. TRITC-fluorescent labeled Control-SPs or Fuco-SPs were retro-orbitally injected 10 min after thrombus initiation with the volume of 150 µL (5 mice per group).

For histological evaluation, mice were sacrificed with pentobarbital overdose 5 min after administration of SPs. The affected part of the mesenteric vein was cut, washed in 0.9% NaCl, fixed in paraformaldehyde 4% (w/v), and frozen. The vein samples were cryosectioned at 10 µm thickness. The cell nuclei of a venous vascular wall were labeled with DAPI (Thermo Fisher Scientific, Massachusetts, United States) contained in a mounting medium (Vecto laboratories). The samples were observed by fluorescence microscopy. For the quantitative analysis, normalized MFI of the TRITC signal from SPs was expressed, defined as total TRITC

fluorescence intensity divided by the size of the thrombus area on 2 slides from each mouse with the ImageJ (NIH, Bethesda, U.S.).

Statistical analysis: Quantitative data were expressed as mean ± standard error of the mean (SEM) ($n \geq 3$). Statistical tests were carried out with GraphPad Prism 9 (GraphPad Software, Inc., La Jolla, U.S.) with a 95% confidence level. Kolmogorov-Smirnov normality test was utilized to examine if variables are normally distributed. Normally distributed data were analyzed then with unpaired t-test or one-way analysis of variance (ANOVA) with post hoc Turkey's test. The Mann-Whitney U test was applied otherwise. The p-values of * $p<0.05$; ** $p<0.01$; *** $p<0.001$ were considered statistically significant.

3. RESULTS

3.1. Submicroparticle synthesis and characterization

Novel polysaccharide SPs were elaborated by a simple and reproducible two-step synthesis process (**Figure 1**A). First, a stable w/o miniemulsion of the aqueous phase with hydrophilic polysaccharides and vegetable (sunflower) oil was prepared. Chemical crosslinking of polysaccharides with the crosslinking agent STMP under alkaline conditions (**Figure 1**B) produced a suspension of uniform SPs. We refer to the hydrogel particles only from dextran as Control-SPs, and from a mixture of dextran and fucoidan as Fuco-SPs in this manuscript.

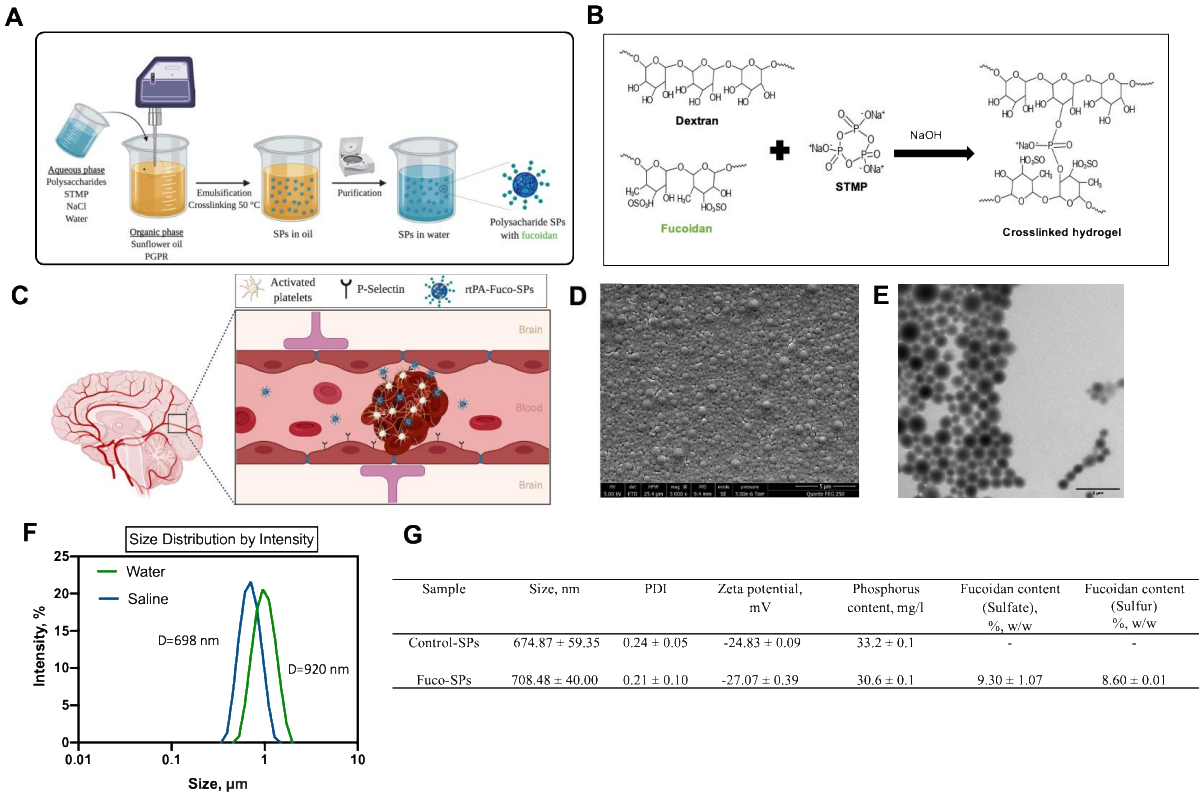

Sample	Size, nm	PDI	Zeta potential, mV	Phosphorus content, mg/l	Fucoidan content (Sulfate), %, w/w	Fucoidan content (Sulfur) %, w/w
Control-SPs	674.87 ± 59.35	0.24 ± 0.05	-24.83 ± 0.09	33.2 ± 0.1	-	-
Fuco-SPs	708.48 ± 40.00	0.21 ± 0.10	-27.07 ± 0.39	30.6 ± 0.1	9.30 ± 1.07	8.60 ± 0.01

Figure 1. Synthesis and physico-chemical characterization of the SPs. A. Overall schematic of the synthesis process of the SPs – miniemulsion / crosslinking. **B.** Crosslinking of the polysaccharides (dextran and fucoidan) with STMP in alkaline conditions. **C.** Proposed therapeutic mode of action of the rtPA-loaded Fuco-SPs after the ischemic stroke: the Fuco-SPs accumulate on the surface of the activated platelets due to P-selectin affinity of fucoidan and perform local thrombolysis with alteplase. SEM **(D)** and TEM **(E)** images of the Fuco-SPs. **F.** Swelling in the water of the Fuco-SPs due to the hydrogel nature of the particles. The size of one sample when resuspended in water (green) and in saline (blue). **G.** Size, zeta potential, and chemical composition of the SPs.

To ensure desirable safety of the future drug delivery platform, a thoughtful approach to material selection was effectuated. Low molecular weight dextran 40 kDa of clinical-grade was utilized without any chemical modification. Having a large number of hydroxyl groups, dextran is a suitable compound for subsequent chemical crosslinking with STMP,[28] an FDA-approved food additive[31] that is preferred over conventional crosslinker glutaraldehyde known for cytotoxicity.[32] Fucoidan, a marine polysaccharide approved as a pharmaceutical compound[33] that exhibits a nanomolar affinity to P-selectin,[34] served as a targeting ligand to thrombi. Hence, both natural polysaccharides applied in this study are affordable,

biodegradable, biocompatible compounds, non-immunogenic, and approved for clinical applications.

Instead of commonly used organic solvents, sunflower oil was applied as an emulsion continuous phase. The choice of the stabilizing agent plays an important role in reducing the interfacial tension and Laplace pressure when fabricating a stable emulsion and future nanocarrier. In this work, we selected a potent oil-soluble nonionic surfactant for stabilizing w/o emulsions – PGPR, which is also recognized by the FDA as a safe compound and is frequently used as an emulsifier in the food production industry.[35] In addition, to counteract the Ostwald ripening of water droplets, 6 M NaCl was added to the aqueous phase as an osmotic agent to adjust the osmotic gradient and to stabilize the w/o emulsion further. Overall, multiple parameters were optimized to obtain a stable and homogenous miniemulsion and subsequent nano-delivery system. It was found that the size of the templating droplet and the ultimate hydrogel SPs being directly proportional to the polysaccharide molecular weight and inversely proportional to the amount of surfactant and crosslinking agent as well as homogenization speed (data not shown).

ESEM and TEM images revealed a well-defined spherical morphology and uniform size distribution of SPs (**Figure 1**D, E). As hydrogel-based particles, they could swell in an aqueous medium while maintaining their network structure (**Figure 1**F).

Functionalized Fuco-SPs contained 8.60 ± 0.01% of fucoidan in a mass of the total SPs weight, determined by elemental analysis of sulfur, and 9.30 ± 1.07% of fucoidan by quantification of the sulfate content by a semi-quantitative colorimetric assay. In such a way, two different techniques estimated ~9% fucoidan composition in the SPs. The physico-chemical properties of these nanoformulations are displayed in **Figure 1**G. The SPs exhibited the hydrodynamic size 674.87 ± 59.35 nm (Control-SPs) and 708.48 ± 40.00 nm (Fuco-SPs), determined by DLS. It is important to highlight that a relatively large size of the SPs might limit

the accumulation of associated rtPA within the brain parenchyma and reduce the risk of hemorrhagic events. The negative ζ-potential of the SPs -24.83 ± 0.09 mV for Control-SPs and -27.07 ± 0.39 mV for Fuco-SPs ensured colloidal stability as a result of the anionic nature of the fucoidan and the formation of the anionic phosphate functional groups, produced during the crosslinking reaction with STMP. The phosphorus content of the SPs is indicated in **Figure 1**G.

The size and zeta potential of both SPs remained relatively stable for at least 30 days at 4 °C. Besides, effective storage of the SPs can be ensured by freeze-drying with 5% (w/v) sucrose as a cryoprotectant and subsequent resuspension in an aqueous medium. The overall yield of the synthesis was 13.4 ± 0.7 mg of SPs.

3.2.Biocompatibility of the SPs

The injectable hydrogel SPs were produced according to the green chemistry principles through the formulation method without using hazardous substances and organic solvents and were expected to be biocompatible.

An initial *in vitro* evaluation of biocompatibility of the developed SPs examined cyto- and hemocompatibility. The cytocompatibility of the SPs was assessed with a resazurin cell viability assay on endothelial cells. Following 24 h exposure, Control-SPs and Fuco-SPs did not affect cellular viability and metabolic activity of HUVECs at concentrations ranging from 0.1 to 1.5 mg/ml, exhibiting an excellent cytocompatible profile (cell survival > 90%, up to the highest tested concentrations of SPs) (**Figure 2**A). The upper limit for the tested concentration 1.5 mg/ml of the SPs was selected to surpass the tested concentrations for the majority of the nanosystems *in vitro* (typically, maximum 400 μg/ml)[36] and the concentration of the SPs employed for further *in vivo* experiments in this work (71 mg SPs per 1 kg body weight or 1.1 mg SPs per 1 mL of blood). There was no significant difference between the Control-SPs and Fuco-SPs, as both did not provoke cytotoxicity.

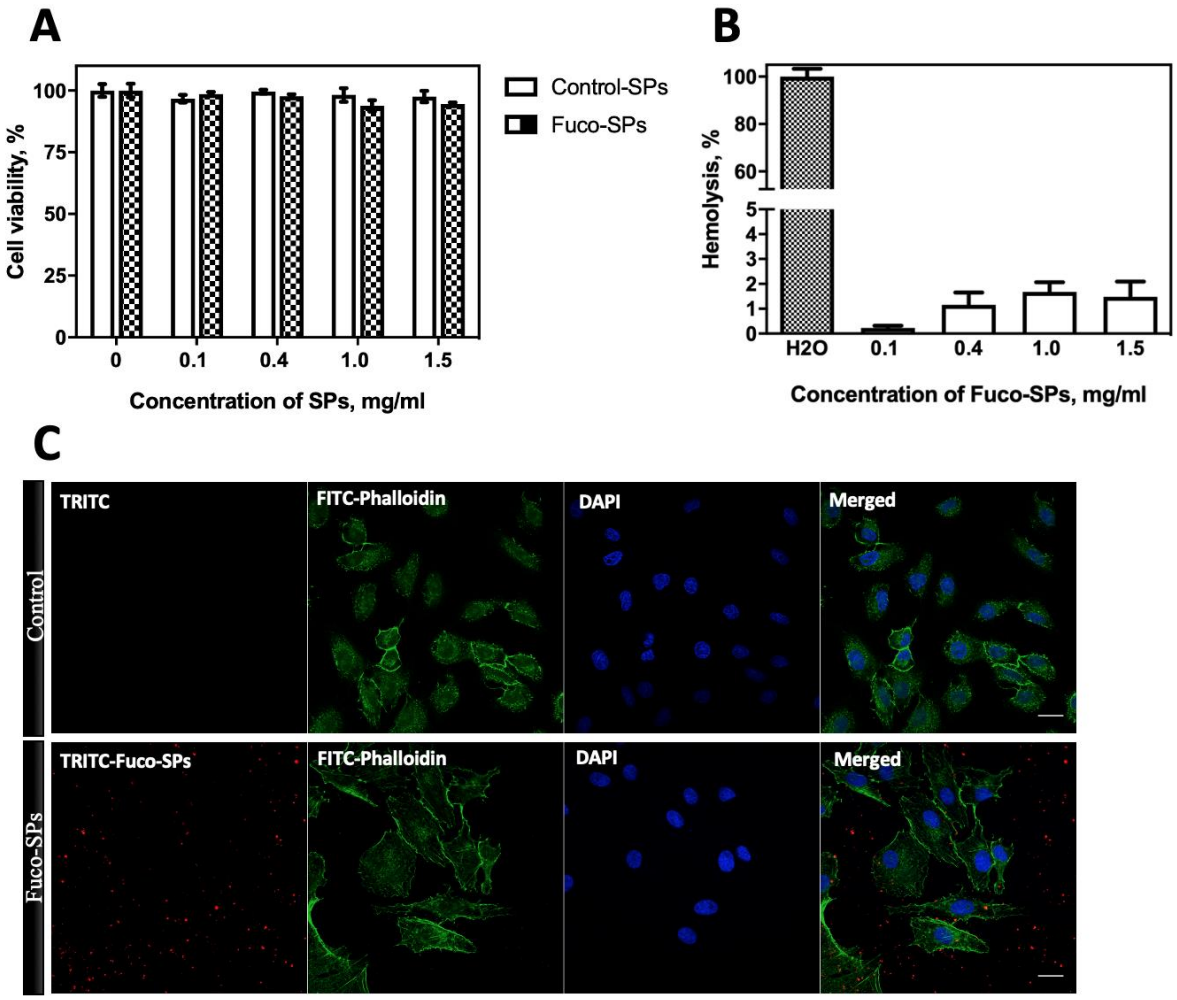

Figure 2. Biocompatibility of the SPs. Cytocompatibility **(A)** and hemocompatibility **(B)**. Confocal microscopy of HUVECs cultured without (control) and with Fuco-SPs **(C)** (scale bar = 30 µm).

Since the SPs in this study were designed for intravenous administration and were expected to have direct contact with blood, the Fuco-SPs were examined for their blood-compatible behavior by a hemolysis test on isolated murine red blood cells *in vitro* (**Figure 2**B). Even at the highest concentration of 1.5 mg/ml, the SPs presented a hemolytic index 1.51 ± 0.02%, below 2%, and considered nonhemolytic according to ISO 10993 - 4 standard.[37,38]

Morphology of the cells, co-cultured with Fuco-SPs, was visualized with confocal microscopy. No obvious morphological differences were revealed for HUVECs with Fuco-SPs and negative control, as depicted in **Figure 2**C. FITC-Phalloidin staining was used to visualize a cytoplasm and DAPI for nuclei. Moreover, the SPs were internalized by endocytosis as the

merged images of all three probes revealed colocalization of the particles within the dye in the cytoplasm.

Collectively, these results suggest that the polysaccharide SPs have favorable biocompatibility for their application *in vivo*.

3.3.Binding of SPs to P-selectin *in vitro*

Knowing that fucoidan was homogeneously distributed in the structure of the hydrogel Fuco-SPs and constituted ~ 9% w/w of the composition, we investigated whether its quantity on the surface was sufficient for specific adhesion to its molecular target. While most of the publications assess targeting strategy *in vitro* in static conditions by flow cytometry or confocal microscopy,[17,39,40] our group developed a robust and tunable dynamic microfluidic method that mimics arterial or venous blood flow conditions to study the targeting efficacy for recombinant P-selectin or/and human activated platelet aggregates expressing P-selectin. It was previously validated on fucoidan-coated nano-/microcarriers (**Figure S1**, Supplementary Data).[18–20]

First, fluorescent Fuco-SPs and Control-SPs were injected in the microchannels coated with recombinant P-selectin under arterial or venous shear rates (67.5 dyne cm^{-2} vs. 6.75 dyne cm^{-2}), and their adhesion was visualized and quantified in real-time under fluorescence microscopy. According to obtained results, fluorescent Fuco-SPs depicted a significantly higher adhesion to P-selectin coating than Control-SPs both in arterial (374.25 ± 115.33 adhered Fuco-SPs vs. 30.25 ± 13.84 adhered Control-SPs, * $p < 0.05$) and venous (228.25 ± 36.67 adhered Fuco-SPs vs. 34.50 ± 18.16 adhered Control-SPs, ** $p < 0.01$) flow conditions (**Figure 3**A, E). There was no significant difference between the fluorescent signal of Fuco-SPs accumulation for arterial and venous flow conditions ($p=0.2731$). Fuco-SPs accumulation after injection onto P-selectin coating was in a linear dose-dependent manner as regards to the P-selectin

concentration, R^2=0.9904 (**Figure 3**B). An experiment of competitive interaction illustrates that fucoidan solution pre-injection at 10 mg/ml considerably reduced the attachment of the Fuco-SPs onto the microchannels with P-selectin (374.25 ± 115.33 vs. 19.75 ± 10.06, * p <0.05) (**Figure 3**C).

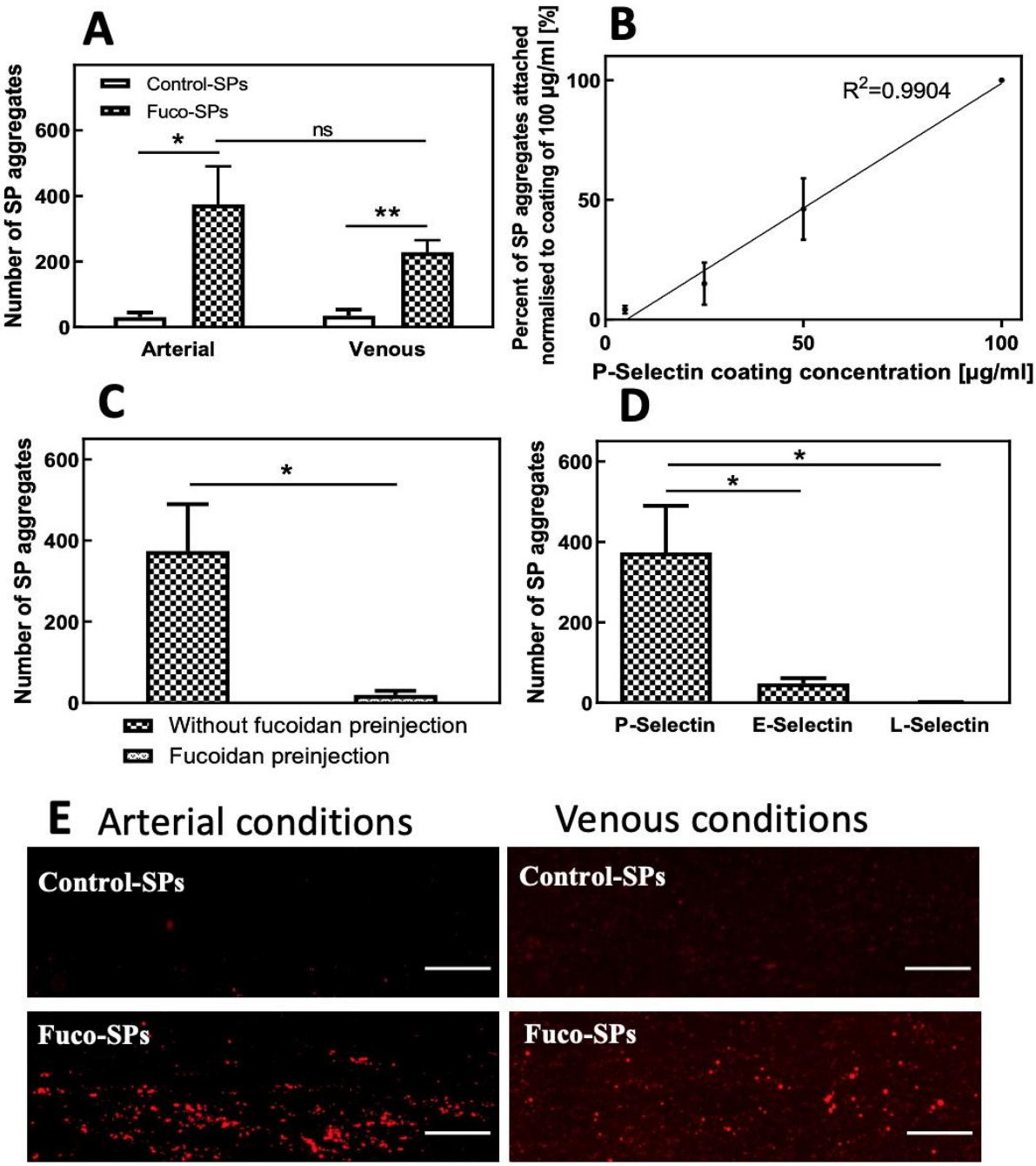

Figure 3. Evaluation of the SPs interactions with selectins. **A.** Adhesion of the Control-SPs or Fuco-SPs on the coating of the recombinant P-selectin in the microfluidic assay under arterial and venous flow conditions (n = 4). **B.** Concentration-dependent binding of the Fuco-SPs onto the coating of the P-selectin at a range of concentrations. **C.** Fucoidan pre-injection inhibited

Fuco-SPs adhesion onto the P-selectin. **D.** Comparison of the Fuco-SPs binding to other selectins: E- and L-Selectin. **E.** Fluorescent microscope view of Control-SPs or Fuco-SPs adhesion over a P-selectin coating of 100 µg/ml under arterial and venous shear rates (scale bar = 20 µm).

To establish the specificity of the Fuco-SPs binding to P-selectin, the targeting assay was extended to other members of the selectin family: E- and L-selectin.[41] The percentage of the Fuco-SPs adhered to the E- and L-selectin was normalized over the mean number of the attached Fuco-SPs to a P-selectin coating at the equivalent concentration. Indeed, only 12.73 ± 3.66% of the SPs adhered to E-selectin and 0.26 ± 0.19% to L-selectin coating (**Figure 3**D). Thus, our results indicate that Fuco-SPs bind specifically to P-selectin but not to E- and L-selectins, and these results are in accordance with a previous work of our group published by Bo L. *et al.* of fucoidan-functionalized polymer microcapsules.[18]

Overall, these findings are encouraging evidence of the sensitivity and selectivity of the Fuco-SPs, confirming fucoidan potential as a natural ligand of P-selectin.

3.4.rtPA loading onto the SPs and its release in saline. *In vitro* thrombolytic activity o rtPA-loaded SPs

Due to rtPA low bioavailability and requirement of high dose administration, coupling this enzyme to the biocompatible nanocarrier could overcome the drawbacks associated with a drug high dosage. Herein, an efficient rtPA encapsulation was achieved through the physical adsorption method due to electrostatic interaction: the protein, which is an amphoteric molecule, was put in contact with negatively charged polysaccharide SPs in the water at pH below rtPA isoelectric point IP=7.7[42,43] when rtPA presented a positive charge. The hydrogel nature of the SPs allowed reaching a high encapsulation efficiency of the rtPA of 64.78 ± 2.16% and 81.04 ± 1.86% for Control-SPs and Fuco-SPs, respectively. The confocal microscopy images of FITC-rtPA loaded onto TRITC-labelled Fuco-SPs revealed the uniform distribution of the rtPA within a porous structure of the hydrogel SPs, as evidenced by a green fluorescence from

FITC-rtPA colocalized with the red fluorescence from the particles (**Figure S2**A, Supplementary Data).

The release kinetics of rtPA from fucoidan-functionalized SPs was analyzed *in vitro* by flow cytometry[44] in saline at 37 °C under gentle agitation by quantifying the MFI of the FITC-labelled rtPA associated with TRITC-fluorescent Fuco-SPs. **Figure S2**B, Supplementary Data indicated a gradual and continuous sustained release of the lytic agent from the SPs during the observation period: 46.41 ± 1.34% of the encapsulated protein was released during the first 15 min, and 76.98 ± 1.74% after 90 min. This release profile is classical for the hydrogels.[45]

The thrombolytic activity of the rtPA-loaded SPs *in vitro* was analyzed as a combination of amidolytic and fibrinolytic activities (**Figure 4**A, B, C). Amidolytic or enzymatic activity featured the ability of the proteolytic enzyme to hydrolyze the rtPA substrate. Interestingly, the amidolytic activities of rtPA on Control-SPs and Fuco-SPs were comparable to that of free rtPA (**Figure 4**A & **4**B). The fibrinolytic experiment *in vitro* of the rtPA-loaded SPs was performed in a fibrin plate assay (**Figure S3**A, Supplementary Data). The results indicated full retention of fibrinolytic activity (**Figure 4**C; **Figure S3**B, Supplementary Data). rtPA loaded onto the SPs appeared to diffuse into the fibrin-agarose matrix and induce fibrinolysis in contact with fibrin. No significant difference was detected between both types of SPs, enabling us to utilize them in the following experiments.

Overall, the rtPA association with the SPs did not affect the drug amidolytic activity and fibrinolytic potential in our design. This result is in accordance with most studies on nanogels suggesting that drug encapsulation via a passive diffusion into the preformed nanogels does not affect the secondary structure of the adsorbed protein and its biological activity.[46]

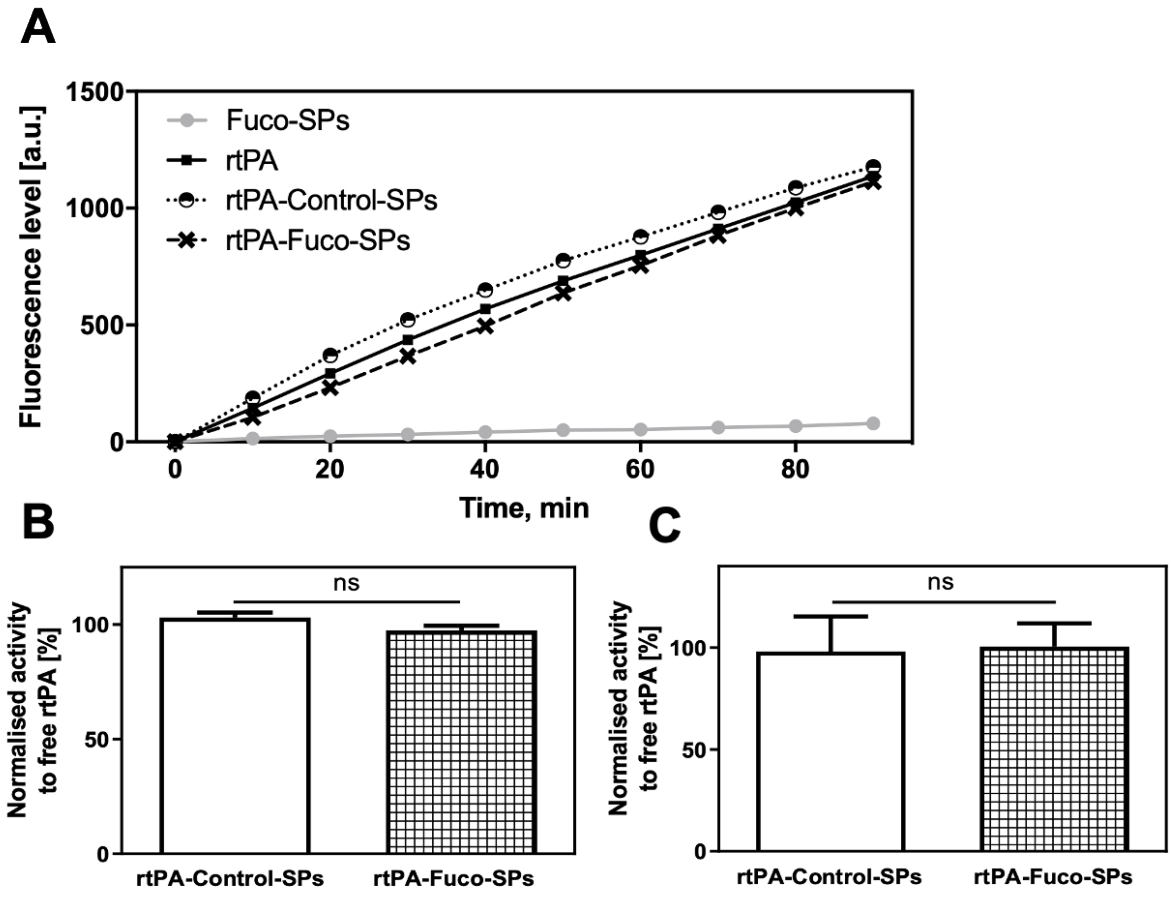

Figure 4. **Thrombolytic efficacy *in vitro* of the rtPA-loaded SPs. A - B.** Amidolytic activity measured by the PefaFluor® fluorogenic assay. **A.** The curves correspond to the mean value of fluorescence release and are correlated to the enzymatic velocity over 90 min. **B.** Corresponding quantitative analysis normalized to free rtPA at the same concentration at 90 min (n=3). **C.** Fibrinolytic activities of the SPs determined by a fibrin-plate agarose assay. The quantitative analysis normalized to free rtPA at the same concentration (n=3).

3.5.Unloaded and rtPA-loaded Fuco-SPs adhere to activated platelet aggregates *in vitro* under arterial flow

Since aggregation of activated platelets and platelet-mediated coagulation pathways are hallmark events in thrombosis, activated platelets are a suitable cellular target for nanocarrier binding to thrombi.[47] Before the *in vivo* tests, we complemented the targeting evaluation on selectins with the second set of microfluidic experiments to validate Fuco-SPs capability to actively anchor onto the surface of activated platelets, expressing P-selectin. Thus, human whole blood was passed into collagen-coated microchannels to induce platelet activation and aggregation. Fuco-SPs or Control-SPs were then perfused at arterial shear stress and the

accumulation of the fluorescence from the adhered SPs was detected on the surface of activated platelet aggregates. A quantitative analysis of the MFI revealed that Fuco-SPs adhered significantly more onto activated platelets than Control-SPs (2,678.34 ± 237.40 for Fuco-SPs vs. 392.44 ± 137.15 for Control-SPs, *** p <0.001, **Figure 5**A & 5B Left). Notably, adsorption of rtPA did not impair the Fuco-SPs clot-binding ability (1,880.80 ± 429.37 for rtPA-Fuco-SPs vs. 77.56 ± 40.25 for rtPA-Control-SPs, ** p <0.01, **Figure 5**B Right). There was no significant difference between unloaded and rtPA-loaded Fuco-SPs adhering to the activated platelets (p=0.1149).

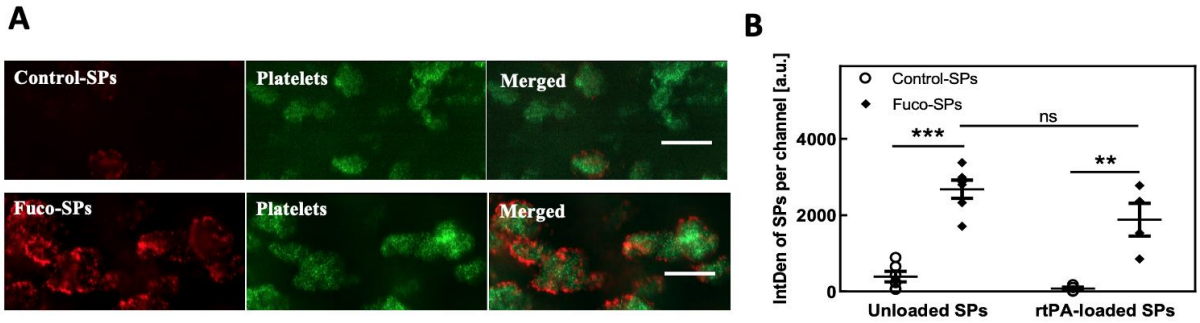

Figure 5. Adhesion of the SPs over activated platelet aggregates. A. Visualization by fluorescent microscopy of the attached unloaded SPs on the microchannels after the formation of the platelet aggregates (scale bar = 20 µm). **B.** Corresponding quantification of the integral density of the unloaded (n=6) and rtPA-loaded (n=4) Control-SPs and Fuco-SPs in ImageJ.

In conclusion, these *in vitro* experiments provided crucial evidence of molecular interaction and high affinity between the P-selectin on the activated platelets and fucoidan-functionalized SPs, which was maintained after loading the thrombolytic agent. This finding presumes that the administration of the rtPA-Fuco-SPs could enable a specific delivery of the rtPA-immobilized SPs to the platelet-rich thrombus with higher drug accumulation.

3.6.Tissue distribution *in vivo* of fucoidan-functionalized SPs

After their intravenous injection, the distribution *in vivo* of Fuco-SPs was examined by histological analysis of the excised tissues with alcian blue staining of negatively charged

particles in the healthy mouse. The presence of Fuco-SPs in four main organs of excretion (liver, spleen, lungs, and kidneys) was assessed on several sections for each organ. Our results revealed that the polysaccharide Fuco-SPs distributed primarily into the spleen post-administration, indicating the splenic clearance. The particles accumulated in the liver to a lower extent, while their presence in the kidneys and lungs remained minor. These differences are presented in **Figure S4**, Supplementary Data. Our data are in agreement with other deformable polymer hydrogel-like particles in their submicron and micron size range.[48]

3.7.*In vivo* thrombolytic efficacy

Whereas demonstrating the *in vitro* activity of the rtPA immobilized on the drug delivery system is important, the *in vivo* therapeutic effect is paramount. A murine thromboembolic stroke model was established by *in situ* injection of 1 IU of thrombin into the MCA by provoking a coagulation cascade and formation of both fibrin- and platelet-rich clots in the lumen of the artery.[49,50] **Figure 6**A highlights the *in vivo* experiments design, and **Figure 1**C the potential mode of action of the Fuco-SPs on the thrombus. The treatment options – control saline, rtPA 10 mg/kg, or rtPA-Fuco-SPs at 10 mg/kg – were intravenously injected 20 min after ischemic onset under rtPA clinical mode of administration: 10% bolus followed by 90% infusion. It is important to note that 10 mg/kg is a relevant dose in mice in place of 0.9 mg/kg in humans because of a lower sensitivity of human rtPA in murine plasma.[51] No morbidity or mortality was observed in the mice during therapeutic experiments, suggesting that rtPA-Fuco-SPs do not provoke acute toxicity under the current conditions.

Cerebral blood flow was monitored throughout the treatment via laser Doppler speckle contrast imaging, a high resolution and high-speed technique that instantly visualizes microcirculatory tissue blood perfusion. The reduction of the blood flow in the ipsilateral cerebral hemisphere due to the stroke was restored by 33.97 ± 5.15% after 40 min treatment

with rtPA-Fuco-SPs; by contrast, in the rtPA and saline group for which the perfusion was improved only by 15.16 ± 6.49% and 10.33 ± 4.62%, respectively, in this experiment (**Figure 6**D). The representative laser Doppler speckle multispectral imaging in the ipsilateral and the contralateral hemispheres at 0 min and 40 min are expressed in **Figure 6**C. Accelerated **Video S1**A, B, C recorded the perfusion in real-time for all conditions. These data were confirmed by the angiographic analysis performed 24 hours later and assessed by a blinded observer based on TICI grade flow scoring measured by magnetic resonance angiography (MRA). Indeed, similar to some untreated stroke patients, the blood clots were gradually lysed post-stroke in this murine model: at 24 h after thrombotic occlusion, 40% of mice exhibited a total recanalization (score 3) and 60% partial perfusion (score 1 and score 2) of the MCA when injected with saline (**Figure 6**G; **Figure S5**A, Supplementary Data). However, after the treatment with rtPA-Fuco-SPs, most of the cases were entirely recanalized (score 3). For the rtPA treated group, no animal achieved a score 1 of minimal perfusion, and 66.6% of cases showed a partial score 2 level of recanalization.

We then utilized magnetic resonance imaging as a powerful technique to quantify the volume of brain damage at 24 hours after stroke onset. Using T2-weighted MRI sequences, we observed that the size of the ischemic brain lesions for the control saline group was 14.80 ± 3.34 mm^3 whereas for the rtPA-loaded fucoidan-targeted SPs it was 4.63 ± 1.59 mm^3 (**Figure 6**E & **6**F). rtPA-conjugated Fuco-SPs reduced the ischemic zone almost 2-fold of the free rtPA, despite the fact that these data were non-significant due to the limited number of the animals as to the well-known effect of free rtPA in this murine model.[50] Out of all treated animals with rtPA-Fuco-SPs, 66.6% of the animals displayed small lesion sizes (<3 mm^3), and 33.3% had medium lesion sizes (<11 mm^3). In the rtPA group, only 33.3% of the animals displayed a small infarct zone. In the saline treatment group, we recorded 60% of the animals with severe (<20

mm^3) and critical (>20 mm^3) lesions and no animals with small lesions (**Figure S5**B, Supplementary Data).

To monitor the BBB integrity disrupted by ischemic stroke,[52] extravasation of gadolinium injected intravenously was detected and quantified on T1-weighted MRI images at day 4 after stroke (**Figure 6**H & **6**I). Gadolinium extravasation from the blood into the brain parenchyma was unmistakably located at the ischemia-affected region where the BBB is compromised. rtPA-Fuco-SPs treatment group demonstrated a significant BBB preservation over control groups of free rtPA and saline with only a subtle BBB breakdown of 3.45 ± 1.40 mm^3.

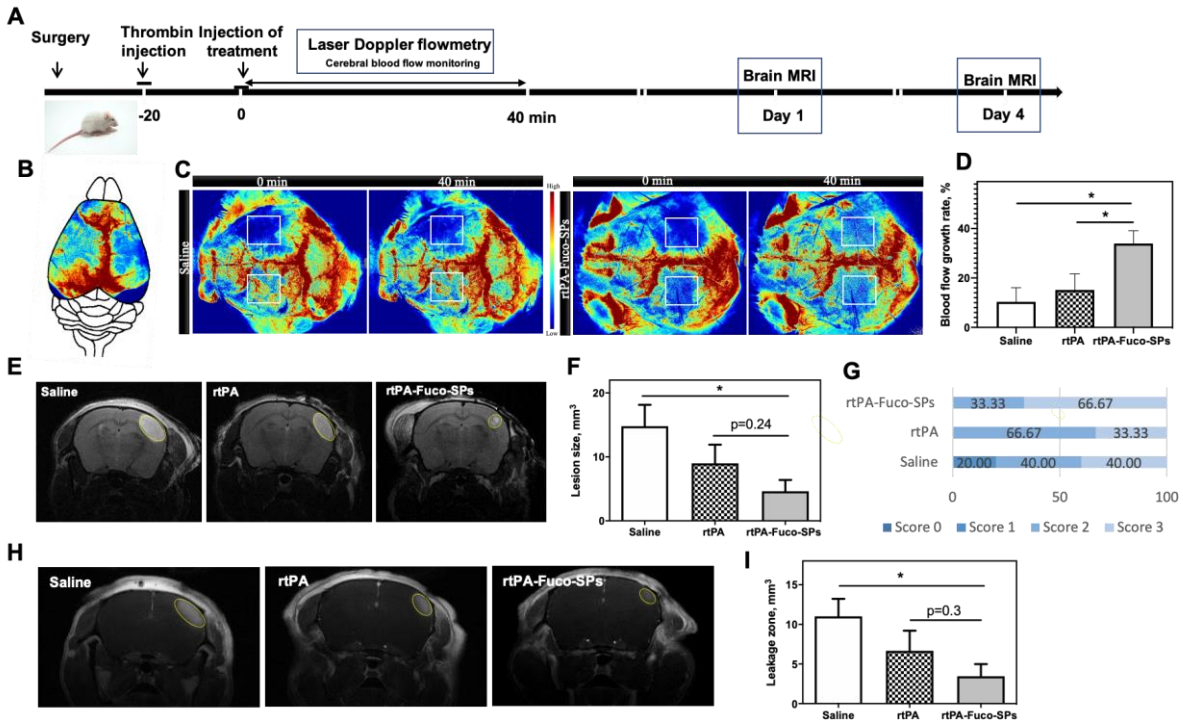

Figure 6. Thrombolytic efficacy *in vivo* in the murine ischemic stroke model. **A.** Schematic of the design of the *in vivo* experiment. **B – D.** Cerebral blood flow reperfusion monitored by the laser speckle contrast imaging during the 40-min treatment (n≥5). Schematic image of the perfusion in the microcirculatory brain tissue. **(B)**. The representative multispectral photos in the ROI of ipsilateral (upper) and contralateral (lower) hemispheres at 0 min and 40 min for saline and rtPA-Fuco-SPs groups **(C)**. The growth rate of the cerebral reperfusion in the ipsilateral hemisphere after 40 min treatment injection **(D)**. **E.** MRI images of the infarct lesion 24 h post-stroke with the corresponding quantification of its volume **(F)**, (n≥5). **G.** Angiographic scores of the MCA reperfusion at day 1 after stroke induction by MRI. **H.** MRI images of the BBB permeability at day 4 post-stroke with the corresponding quantification of its volume **(I)**, (n≥5).

In order to confirm the accumulation of Fuco-SPs within the thrombus area *in vivo*, we injected fluorescent-labeled SPs at the therapeutic concentration as in the stroke model into the $FeCl_3$ model of venous thrombosis in mice. Upon histological examination of the thrombus-affected area of the mesenteric vein, Fuco-SPs were clearly identified on the green-fluorescent labeled thrombus **(Figure 7**A**)**. By a quantitative analysis of the MFI normalized by the size of the thrombus, it was evidenced a highly increased TRITC signal from fucoidan-functionalized SPs group comparing with Control-SPs (9.48 ± 2.19 for Fuco-SPs vs. 1.48 ± 0.35 for Control-SPs, ** p <0.01, **Figure 7**B).

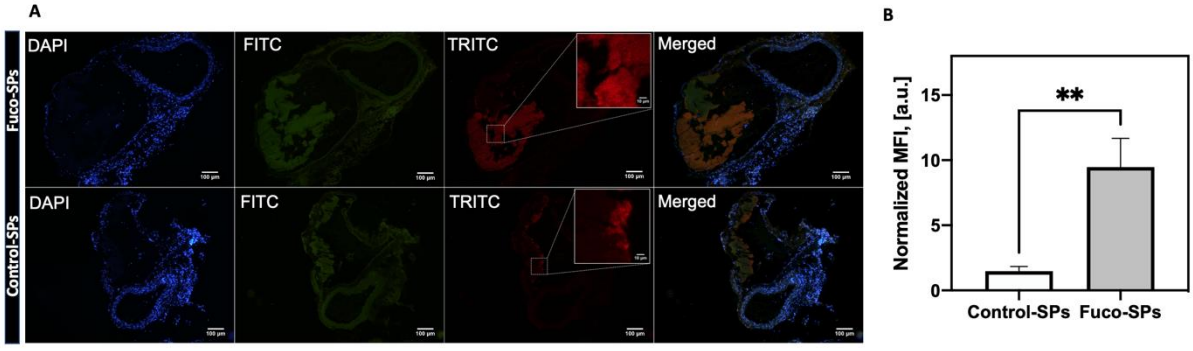

Figure 7. *In vivo* targeting in the $FeCl_3$ murine model of thrombosis. A. Histological analysis of thrombi in the mesenteric vein by fluorescent microscopy. The venous vascular wall is visualized with DAPI staining; thrombus is stained in green due to DIOC6 labeling of platelets; Fuco-SPs and Control-SPs are fluorescently labeled with TRITC. Inserts are a magnification of dashed Regions of Interest of the TRITC signal. **B.** Corresponding quantification of MFI from the adhered TRITC-SPs in the thrombi (n=5).

Overall, the apparent superiority of rtPA-Fuco-SPs to reduce the brain tissue injury area in comparison with saline and rtPA at the same dose, combined with a favorable safety profile of the SPs, makes them a promising nanomedicine-based approach for the treatment of acute arterial thrombosis.

4. DISCUSSION

The revolutionary treatment with alteplase to dissolve thrombi and restore blood flow is a standard of care in acute thrombotic events, but it is certainly not risk-free. Nanomedicine exploits a profound understanding of the molecular mechanisms involved in thrombus

formation and offers outside-the-box strategies to effectively target and dissolve the blood clots in the body with fewer systemic and neurological complications.[53]

In this study, rtPA was associated with hydrogel-like polysaccharide SPs, synthesized by a simple and reproducible miniemulsion / crosslinking process. The soft structure of chemically crosslinked hydrogels resembles those of extracellular matrices and may prevent tissue irritation, providing a convenient and versatile platform for storage and site-specific delivery of a drug to the thrombi.[54] Our approach's novelty is exclusively polysaccharide nature of the particles – from dextran and fucoidan without any chemical modification, as well as green chemistry synthesis technique. Intriguingly, several articles claim that dextran[55] and fucoidan[56,57] themselves exert some antithrombotic action that makes them an excellent starting material for the nanocarrier. Hydrophilic polysaccharide surfaces lead to longer circulating NPs since they avert the formation of a protein corona and early macrophage internalization.[58] Moreover, natural polysaccharides are advantageous to synthetic polymers in terms of safety, abundance in nature, and low cost. Overall, we considered the issues imperative for high biosafety and potential future clinical translation of Fuco-SPs by (I) the choice of biocompatible and biodegradable materials, all with FDA-approval; (II) a relatively simple and efficient production by a mild synthesis method without the utilization of the hazardous substances and organic solvents; (III) targeting agent of natural origin– fucoidan – that is being validated in clinical trials for thrombosis.

After fabrication and extensive physico-chemical characterization of the SPs, we confirmed their cyto- and hemocompatibility at concentrations up to 1.5 mg/ml (**Figure 2**A & 3B). The main pathway of the polysaccharide Fuco-SPs tissue distribution *in vivo* upon intravenous injection was the spleen (**Figure S4**, Supplementary Data). Future studies should include the tests of thrombogenicity and immunogenicity *in vivo*.

The Fuco-SPs were associated with a thrombolytic agent by physical adsorption, allowing a high encapsulation efficiency of the rtPA of 81.04 ± 1.86% due to their hydrogel-based structure. Classically, alteplase is loaded onto the NPs using the covalent amide bond formation via EDC/NHS reaction between the primary amines on the rtPA molecule and the nanocarriers containing carboxyl groups. As a mild drug encapsulation method, adsorption is preferred to covalent bioconjugation to load fragile molecules such as proteins to avoid changes in the protein structure and function that might result in its partial denaturation and loss of biological activity.[59] The fibrinolytic diffused through the matrix of the porous SPs (**Figure S2**A, Supplementary Data), fully preserving its enzymatic and fibrinolytic potential *in vitro* (**Figure 4**). Friedrich *et al*. demonstrated that the adsorptive bound rtPA liberated faster from the particles and spread more readily into the fibrin matrix than covalently bound rtPA,[60] which may be beneficial in targeted thrombolysis. Although a rising number of recent articles apply a controlled release of the thrombolytics via endogenous and exogenous stimuli, we chose not to incorporate sophisticated nanodesigns and demonstrated a gradual and continuous rtPA release from the SPs without an external trigger (**Figure S2**B, Supplementary Data) so as to facilitate future regulatory approvals.

The clot targeting strategy of the SPs was achieved by the introduction of the fucoidan to the polysaccharide solution at 9% w/w. Functionalization with fucoidan permitted the high-affinity binding of Fuco-SPs to its molecular target P-selectin in a dynamic microfluidic method that mimics arterial or venous blood flow conditions in a dose-dependent manner (**Figure 3**A-B, AE). Importantly, this type of interaction is selective, as SPs did not adhere to other selectins: E- and L-selectin *in vitro* (**Figure 3**D). When the microchannels were covered with activated platelet aggregates, both unloaded and rtPA-loaded Fuco-SPs were capable of binding these micro-clots (**Figure 5**). Once tested in the *in vivo* model of venous thrombosis, Fuco-SPs were identified on the $FeCl_3$-induced thrombi by histological examination, contrary to Control-SPs

(**Figure 7**). Our data validate an inimitable and efficient thrombus targeting approach of the Fuco-SPs, using a clinical algae-derived compound. Yet, a surge in strategies involving dual or even more surface targeting moieties is being witnessed in academic works. For instance, the combinatory targeting of GPIIb/IIIa receptors and P-selectin on activated platelets with two peptide ligands on the lipid nanovesicles enhanced thrombus binding capacities in a synergic manner.[61] Another notable example is the biomimetic functionalization of NPs with platelet membrane coating that enabled thrombus directing via multiple platelet receptors.[62] These combinations of NP modifications represent a promising strategy for developing next-generation blood clot-targeting NP platforms for therapy and/or diagnostics.

The experiments on the murine thrombin-induced thromboembolic stroke model supported the therapeutic effect of the rtPA-Fuco-SPs *in vivo* (**Figure 6**). The findings of the submicroparticle-associated rtPA treatment group outperformed those of free rtPA at the same concentration, as we observed a more rapid clot dissolution and MCA reperfusion, which minimized the brain injury and resulted in subsequently smaller infarct area post-stroke by MRI. The prevailing method for assessing the brain infarct volume is a brain tissue staining with 2% 2,3,5-triphenyltetrazolium chloride (TTC), which labels non-injured tissue and leaves the infarct area white. Several groups previously reported the reduction of the infarct zone in preclinical models by nanomedicinal product. For example, the magnetic iron oxide (Fe_3O_4)-microrods[63] and polyacrylic acid-stabilized magnetic NPs[64] conjugated with rtPA diminished the brain infarct lesion in the $FeCl_3$ murine model of ischemic stroke of MCA. These designs, however, require an external magnet for targeting and to complement chemical lysis with rtPA with mechanical one of the magnetic rotations. Without any clinically approved medical device to impose a high magnetic force on the NPs in deep blood vessels, it would probably be desirable for nanocarrier formulation to avoid external assistance. Mei *et al.* stated that only the synergistic effect of rtPA-loaded polymer micelles and a reactive oxygen species

(ROS)-eliminating antioxidant suppressed an infarct volume and improved neurological deficit after brain ischemia in the mouse model of photo-thrombotic MCA occlusion.[65] In our case, the therapeutic benefit of rtPA-Fuco-SPs could be ascribed to faster MCA reperfusion and, hence, prevention of the major brain injury due to higher rtPA accumulation on the thrombus site as to active targeting and specific P-selectin interactions of the Fuco-SPs.

Moreover, the animals in the rtPA-Fuco-SPs group suffered a lower level of BBB disruption by the ischemic stroke that was quantified on T1-weighted MRI images with gadolinium. It is vital to underline that although in this article we utilized fucoidan on the SPs purely for the P-selectin targeting purpose, new avenues of research are deciphering its neuroprotective role, particularly after cerebral ischemic events.[66] Altogether, this first proof-of-concept *in vivo* results of Fuco-SPs show an astonishing potential of the nanomedicine-based approach for the targeted treatment of acute thrombosis. We speculate that the submicron size of the particles, along with their active thrombus-targeting moiety, should maintain rtPA-loaded nanocarrier within the intravascular compartment to exert its thrombolytic activity. It should prevent the leakage of rtPA into the brain parenchyma, reducing the risks of NMDA receptors-mediated neurotoxicity and hemorrhages.[67] Further studies could compare a single or a double bolus route of administration of rtPA-Fuco-SPs due to the rtPA preservation by SPs, and, thus, a more comfortable treatment option for patients.

Nevertheless, as none of the available *in vivo* rodent experimental models of acute thrombosis accurately recapitulates all the aspects of human disease progression and heterogeneity, it is recommended to validate any translational concept in multiple models to ensure its therapeutic efficacy and safety. Notably, in 2019, Xu *et al.* proposed a biomimetic strategy of platelet membrane-camouflaged PLGA NPs with rtPA that was studied in several *in vivo* models: pulmonary embolism, $FeCl_3$-induced arterial thrombosis, and ischemic stroke model.[62]

Due to technical challenges and strict regulatory requirements, the clinical translation of the nanopharmaceutical products happens slowly. The rtPA-Fuco-SPs representing an actively targeted nanodelivery system reach a balance of safety, simplicity, and functionality concerning the projected clinical application. While they were designed and fabricated in the academic laboratory at the range of ~10 mg per batch, the industrial scale-up of the process with high reproducibility under GMP conditions and intended quality standards is essential to establish in order to obtain the necessary amounts for further screening and, ultimately, clinical use. For instance, high-precision microfluidic and micropatterning methods for the fabrication of monodisperse NPs with uniform physicochemical characteristics and low batch-to-batch variability are becoming prevalent and are compatible with GMP standards.[68] Finally, an adequate sterilization method should be validated to prevent nanoparticle damage and alteration in the product's parameters.

5. CONCLUSIONS

In the present study, we designed and fabricated fucoidan-functionalized 100% polysaccharide submicroparticles from biocompatible and FDA approved components as a P-selectin targeting drug delivery system for thrombolytic therapy. The physico-chemical properties and a biocompatibility analysis of these SPs were thoroughly evaluated, and alteplase was effectively immobilized onto the SPs with full retention of its enzymatic and fibrinolytic potential *in vitro* and sustained drug-release kinetics. We established *in vitro* by dynamic flow microchamber assays that the fucoidan-functionalized nanosystem specifically adhered to the recombinant P-selectin in a dose-dependent manner, but not to E- and L-Selectins, and to human activated platelets. In $FeCl_3$ model of thrombosis, Fuco-SPs accumulated in the thrombus. Finally, our findings revealed in the murine model of ischemic stroke that rtPA conjugation to the Fuco-SPs could enhance the thrombolytic activity of the clinical agent *in vivo*. The blood flow perfusion

was restored more rapidly, which resulted in smaller post-ischemic cerebral infarct lesions and higher BBB protection. In summary, an alteplase-associated hydrogel-based nano-delivery system with fucoidan demonstrates a solid argument for improved thrombolytic therapy in terms of safety and efficacy in the preclinical studies. In future research, our biocompatible Fuco-SPs could also vehicle other therapeutic and/or molecular imaging agents in the vascular compartment to target P-selectin overexpressed pathologies, such as cardiovascular diseases[69] or some cancers.[70,71]

Acknowledgments
The authors would like to acknowledge Marie-Françoise Bricot from the Institut de Chimie des Substances Naturelles of the Université Paris-Saclay for performing a microanalysis of the fucoidan and the Fuco-SPs. We also thank the ImagoSeine core facility of the Institut Jacques Monod, a member of IBiSA and France-Bio-Imaging (ANR-10-INBS-04) infrastructures for the TEM. The authors are grateful for Christine Choqueux, who performed the Environmental SEM at Université de Technologie de Compiègne, Compiègne, France. We kindly thank Pr. Antonino Nicoletti for his advice on designing an *in vitro* release study and Dr. Kevin Guedj for assistance with flow cytometry. We also thank Dr. Yoann Lalatonne for the technical support with the TXRF technique and Dr. Samira Benadda with confocal microscopy. The illustrations were designed with BioRender software (biorender.com). **Funding**: The authors thank INSERM, Université de Paris, and Université Sorbonne Paris Nord for financial support. This work also received funding from the EU project FP7-NMP-2012-LARGE-6-309820 "NanoAthero" and ANR-13-LAB1-0005-01 "FucoChem". Alina Zenych is grateful for the Ph.D. fellowship from the INSPIRE program of the European Union's Horizon 2020 research and innovation program (Marie Sklodowska-Curie grant # 665850).

Author contributions
A.Z.: Conceptualization; Investigation; Data Curation; Formal analysis; Writing - Original Draft; Visualization. C.J.: Investigation (Thrombolytic efficacy *in vivo*). R.A.: Investigation (Tissue distribution *in vivo* & thrombus targeting *in vivo*); Validation. L.F.: Investigation (Quantification of the fucoidan & fibrinolytic activity *in vitro*). L.M.F.R.: Methodology. T.B.: Methodology; Investigation (Thrombolytic efficacy *in vivo* - MRI); Validation; Writing - Review & Editing. D.V.: Resources; Project administration; Writing - Review & Editing. D.L.: Resources; Project administration. C.C.: Conceptualization; Validation; Resources; Writing - Review & Editing; Supervision; Project administration; Funding acquisition. All the authors approved the final version of the manuscript.

Conflict of interests
The authors declare no competing interests.

REFERENCES

[1] E.J. Benjamin, P. Muntner, A. Alonso, M.S. Bittencourt, C.W. Callaway, A.P. Carson, A.M. Chamberlain, A.R. Chang, S. Cheng, S.R. Das, F.N. Delling, L. Djousse, M.S.V. Elkind, J.F. Ferguson, M. Fornage, L.C. Jordan, S.S. Khan, B.M. Kissela, K.L. Knutson, T.W. Kwan, D.T. Lackland, T.T. Lewis, J.H. Lichtman, C.T. Longenecker, M.S. Loop, P.L. Lutsey, S.S. Martin, K. Matsushita, A.E. Moran, M.E. Mussolino, M. O'Flaherty, A. Pandey, A.M. Perak, W.D. Rosamond, G.A. Roth, U.K.A. Sampson, G.M. Satou, E.B. Schroeder, S.H. Shah, N.L. Spartano, A. Stokes, D.L. Tirschwell, C.W. Tsao, M.P. Turakhia, L.B. VanWagner, J.T. Wilkins, S.S. Wong, S.S. Virani, Heart Disease and Stroke Statistics—2019 Update: A Report From the American Heart Association, Circulation. (2019). doi:10.1161/CIR.0000000000000659.

[2] W.J. Powers, A.A. Rabinstein, T. Ackerson, O.M. Adeoye, N.C. Bambakidis, K. Becker, J. Biller, M. Brown, B.M. Demaerschalk, B. Hoh, E.C. Jauch, C.S. Kidwell, T.M. Leslie-Mazwi, B. Ovbiagele, P.A. Scott, K.N. Sheth, A.M. Southerland, D. V. Summers, D.L. Tirschwell, Guidelines for the Early Management of Patients With Acute Ischemic Stroke: 2019 Update to the 2018 Guidelines for the Early Management of Acute Ischemic Stroke: A Guideline for Healthcare Professionals From the American Heart Association/American Stroke , Stroke. 50 (2019) e344–e418. doi:10.1161/STR.0000000000000211.

[3] J. Mican, M. Toul, D. Bednar, J. Damborsky, Structural Biology and Protein Engineering of Thrombolytics, Comput. Struct. Biotechnol. J. 17 (2019) 917–938. doi:10.1016/j.csbj.2019.06.023.

[4] R. Bhatia, M.D. Hill, N. Shobha, B. Menon, S. Bal, P. Kochar, T. Watson, M. Goyal, A.M. Demchuk, Low rates of acute recanalization with intravenous recombinant tissue plasminogen activator in ischemic stroke: Real-world experience and a call for action, Stroke. 41 (2010) 2254–2258. doi:10.1161/STROKEAHA.110.592535.

[5] A.M. Thiebaut, M. Gauberti, C. Ali, S. Martinez De Lizarrondo, D. Vivien, M. Yepes, B.D. Roussel, The role of plasminogen activators in stroke treatment: fibrinolysis and beyond, Lancet Neurol. 17 (2018) 1121–1132. doi:10.1016/S1474-4422(18)30323-5.

[6] A. Pal Khasa, Y. Pal Khasa, The evolution of recombinant thrombolytics: Current status and future directions, Bioengineered. 8 (2017) 331–358. doi:10.1080/21655979.2016.1229718.

[7] S. Liu, X. Feng, R. Jin, G. Li, Tissue plasminogen activator-based nanothrombolysis for ischemic stroke, Expert Opin Drug Deliv. 15 (2018) 173–184. doi:10.1080/17425247.2018.1384464.

[8] N. Korin, M. Kanapathipillai, B.D. Matthews, M. Crescente, A. Brill, T. Mammoto, K. Ghosh, S. Jurek, S.A. Bencherif, D. Bhatta, A.U. Coskun, C.L. Feldman, D.D. Wagner, D.E. Ingber, Shear-Activated Nanotherapeutics for Drug Targeting to Obstructed Blood Vessels, Science (80-.). 337 (2012) 738–742. doi:10.1126/science.1217815.

[9] M. Colasuonno, A.L. Palange, R. Aid, M. Ferreira, H. Mollica, R. Palomba, M. Emdin, M. Del Sette, C. Chauvierre, D. Letourneur, P. Decuzzi, Erythrocyte-Inspired Discoidal Polymeric Nanoconstructs Carrying Tissue Plasminogen Activator for the Enhanced Lysis of Blood Clots, ACS Nano. 12 (2018) 12224–12237. doi:10.1021/acsnano.8b06021.

[10] J. Zhou, D. Guo, Y. Zhang, W. Wu, H. Ran, Z. Wang, Construction and evaluation of Fe3O4-based PLGA nanoparticles carrying rtPA used in the detection of thrombosis and in targeted thrombolysis, ACS Appl. Mater. Interfaces. 6 (2014) 5566–5576. doi:10.1021/am406008k.

[11] A. Friedman, S. Claypool, R. Liu, The Smart Targeting of Nanoparticles, Curr. Pharm.

Des. 19 (2013) 6315–6329. doi:10.2174/13816128113199990375.
[12] W. jin Jeong, J. Bu, L.J. Kubiatowicz, S.S. Chen, Y.S. Kim, S. Hong, Peptide–nanoparticle conjugates: a next generation of diagnostic and therapeutic platforms?, Nano Converg. 5 (2018) 1–18. doi:10.1186/s40580-018-0170-1.
[13] L. Chollet, P. Saboural, C. Chauvierre, J.-N. Villemin, D. Letourneur, F. Chaubet, Fucoidans in Nanomedicine, Mar. Drugs. 14 (2016) 1–24. doi:10.3390/md14080145.
[14] L. Bachelet, I. Bertholon, D. Lavigne, R. Vassy, M. Jandrot-Perrus, F. Chaubet, D. Letourneur, Affinity of low molecular weight fucoidan for P-selectin triggers its binding to activated human platelets, Biochim. Biophys. Acta - Gen. Subj. 1790 (2009) 141–146. doi:10.1016/j.bbagen.2008.10.008.
[15] P. Saboural, F. Chaubet, F. Rouzet, F. Al-Shoukr, R. Ben Azzouna, N. Bouchemal, L. Picton, L. Louedec, M. Maire, L. Rolland, G. Potier, D. Le Guludec, D. Letourneur, C. Chauvierre, Purification of a low molecular weight fucoidan for SPECT molecular imaging of myocardial infarction, Mar. Drugs. 12 (2014) 4851–4867. doi:10.3390/md12094851.
[16] T. Bonnard, J.-M. Serfaty, C. Journé, B. Ho Tin Noe, D. Arnaud, L. Louedec, M. Derkaoui, D. Letourneur, C. Chauvierre, C. Le Visage, Leukocyte mimetic polysaccharide microparticles tracked in vivo on activated endothelium and in abdominal aortic aneurysm, Acta Biomater. 10 (2014) 3535–3545. doi:10.1016/j.actbio.2014.04.015.
[17] T. Bonnard, G. Yang, A. Petiet, V. Ollivier, O. Haddad, D. Arnaud, L. Louedec, L. Bachelet-Violette, S.M. Derkaoui, D. Letourneur, C. Chauvierre, C. Le Visage, Abdominal Aortic Aneurysms Targeted by Functionalized Polysaccharide Microparticles: a new Tool for SPECT Imaging, Theranostics. 4 (2014) 592–603. doi:10.7150/thno.7757.
[18] B. Li, M. Juenet, R. Aid-Launais, M. Maire, V. Ollivier, D. Letourneur, C. Chauvierre, Development of Polymer Microcapsules Functionalized with Fucoidan to Target P-Selectin Overexpressed in Cardiovascular Diseases, Adv. Healthc. Mater. 6 (2017) 1–11. doi:10.1002/adhm.201601200.
[19] B. Li, R. Aid-Launais, M.-N. Labour, A. Zenych, M. Juenet, C. Choqueux, V. Ollivier, O. Couture, D. Letourneur, C. Chauvierre, Functionalized polymer microbubbles as new molecular ultrasound contrast agent to target P-selectin in thrombus, Biomaterials. 194 (2019) 139–150. doi:10.1016/j.biomaterials.2018.12.023.
[20] M. Juenet, R. Aid-Launais, B. Li, A. Berger, J. Aerts, V. Ollivier, A. Nicoletti, D. Letourneur, C. Chauvierre, Thrombolytic therapy based on fucoidan-functionalized polymer nanoparticles targeting P-selectin, Biomaterials. 156 (2018) 204–216. doi:10.1016/j.biomaterials.2017.11.047.
[21] C. Chauvierre, D. Letourneur, The European project NanoAthero to fight cardiovascular diseases using nanotechnologies, Nanomedicine (Lond). 10 (2015) 3391–3400. doi:10.2217/nnm.15.170.
[22] K.H. Zheng, Y. Kaiser, E. Poel, H. Verberne, J. Aerts, F. Rouzet, E. Stroes, D. Letourneur, C. Chauvierre, 99Mtc-Fucoidan As Diagnostic Agent For P-Selectin Imaging: First-In-Human Evaluation (Phase I), Atherosclerosis. 287 (2019) e143. doi:10.1016/j.atherosclerosis.2019.06.425.
[23] I. Cicha, C. Chauvierre, I. Texier, C. Cabella, J.M. Metselaar, J. Szebeni, L. Dézsi, C. Alexiou, F. Rouzet, G. Storm, E. Stroes, D. Bruce, N. MacRitchie, P. Maffia, D. Letourneur, From design to the clinic: Practical guidelines for translating cardiovascular nanomedicine, Cardiovasc. Res. 114 (2018) 1714–1727. doi:10.1093/cvr/cvy219.
[24] K. Ganguly, K. Chaturvedi, U.A. More, M.N. Nadagouda, T.M. Aminabhavi, Polysaccharide-based micro/nanohydrogels for delivering macromolecular therapeutics,

J. Control. Release. 193 (2014) 162–173. doi:10.1016/j.jconrel.2014.05.014.
[25] J. Zhang, W. Xia, P. Liu, Q. Cheng, T. Tahirou, W. Gu, B. Li, Chitosan modification and pharmaceutical/biomedical applications, Mar. Drugs. 8 (2010) 1962–1987. doi:10.3390/md8071962.
[26] H.J. Jin, H. Zhang, M.L. Sun, B.G. Zhang, J.W. Zhang, Urokinase-coated chitosan nanoparticles for thrombolytic therapy: Preparation and pharmacodynamics in vivo, J. Thromb. Thrombolysis. 36 (2013) 458–468. doi:10.1007/s11239-013-0951-7.
[27] J. Liao, X. Ren, B. Yang, H. Li, Y. Zhang, Z. Yin, Targeted thrombolysis by using c-RGD-modified N,N,N-Trimethyl Chitosan nanoparticles loaded with lumbrokinase, Drug Dev. Ind. Pharm. 45 (2019) 88–95. doi:10.1080/03639045.2018.1522324.
[28] S.R. Van Tomme, W.E. Hennink, Biodegradable dextran hydrogels for protein delivery applications, Expert Rev. Med. Devices. 4 (2007) 147–164. doi:10.1586/17434440.4.2.147.
[29] J.R. McCarthy, I.Y. Sazonova, S.S. Erdem, T. Hara, B.D. Thompson, P. Patel, I. Botnaru, C.P. Lin, G.L. Reed, R. Weissleder, F.A. Jaffer, Multifunctional nanoagent for thrombus-targeted fibrinolytic therapy, Nanomedicine (Lond). 7 (2012) 1017–1028. doi:10.2217/nnm.11.179.
[30] S. Heid, H. Unterweger, R. Tietze, R.P. Friedrich, B. Weigel, I. Cicha, D. Eberbeck, A.R. Boccaccini, C. Alexiou, S. Lyer, Synthesis and Characterization of Tissue Plasminogen Activator-Functionalized Superparamagnetic Iron Oxide Nanoparticles for Targeted Fibrin Clot Dissolution, Int. J. Mol. Sci. 18 (2017). doi:10.3390/ijms18091837.
[31] T.E. Furia, CRC Handbook of Food Additives, Second Edi, CRC Press, 1973.
[32] W.E. Hennink, C.F. van Nostrum, Novel crosslinking methods to design hydrogels, Adv. Drug Deliv. Rev. 54 (2002) 13–36. doi:10.1016/S0169-409X(01)00240-X.
[33] C. Chauvierre, R. Aid-Launais, J. Aerts, M. Maire, L. Chollet, L. Rolland, R. Bonaf, S. Rossi, S. Bussi, C. Cabella, D. Laszlo, T. Fülöp, J. Szebeni, Y. Chahid, K.H. Zheng, E.S.G. Stroes, D. Le Guludec, F. Rouzet, D. Letourneur, Pharmaceutical Development and Safety Evaluation of a GMP-Grade Fucoidan for Molecular Diagnosis of Cardiovascular Diseases, Mar. Drugs. 17 (2019) 1–17. doi:https://doi.org/10.3390/md17120699.
[34] F. Rouzet, L. Bachelet-Violette, J.-M. Alsac, M. Suzuki, A. Meulemans, L. Louedec, A. Petiet, M. Jandrot-Perrus, F. Chaubet, J.-B. Michel, D. Le Guludec, D. Letourneur, Radiolabeled fucoidan as a P-selectin targeting agent for in vivo imaging of platelet-rich thrombus and endothelial activation., J. Nucl. Med. 52 (2011) 1433–1440. doi:10.2967/jnumed.110.085852.
[35] F. Wolf, K. Koehler, H.P. Schuchmann, Stabilization of water droplets in oil with PGPR for use in oral and dermal applications, J. Food Process Eng. 36 (2013) 276–283. doi:10.1111/j.1745-4530.2012.00688.x.
[36] J. Matuszak, J. Baumgartner, J. Zaloga, M. Juenet, A.E. da Silva, D. Franke, G. Almer, I. Texier, D. Faivre, J.M. Metselaar, F.P. Navarro, C. Chauvierre, R. Prassl, L. Dézsi, R. Urbanics, C. Alexiou, H. Mangge, J. Szebeni, D. Letourneur, I. Cicha, Nanoparticles for intravascular applications: physicochemical characterization and cytotoxicity testing, Nanomedicine. 11 (2016) 597–616. doi:10.2217/nnm.15.216.
[37] M. Weber, H. Steinle, S. Golombek, L. Hann, C. Schlensak, H.P. Wendel, M. Avci-Adali, Blood-Contacting Biomaterials: In Vitro Evaluation of the Hemocompatibility, Front. Bioeng. Biotechnol. 6 (2018) 99. doi:10.3389/fbioe.2018.00099.
[38] ISO 10993-4:2017, Biol. Eval. Med. Devices — Part 4 Sel. Tests Interact. with Blood. (2017). https://www.iso.org/standard/63448.html.
[39] B. Vaidya, G.P. Agrawal, S.P. Vyas, Platelets directed liposomes for the delivery of streptokinase: Development and characterization, Eur. J. Pharm. Sci. 44 (2011) 589–594.

doi:10.1016/j.ejps.2011.10.004.
[40] N. Zhang, C. Li, D. Zhou, C. Ding, Y. Jin, Q. Tian, X. Meng, K. Pu, Y. Zhu, Cyclic RGD functionalized liposomes encapsulating urokinase for thrombolysis, Acta Biomater. (2018). doi:10.1016/j.actbio.2018.01.038.
[41] K. Ley, The role of selectins in inflammation and disease, Trends Mol. Med. 9 (2003) 263–268. doi:10.1016/S1471-4914(03)00071-6.
[42] J.-H. Kim, J.-Y. Yoon, Protein adsorption on polymer particles, in: Encycl. Surf. Colloid Sci., 2002: pp. 4373–4381. doi:10.1002/jbm.820210202.
[43] I. Politis, L. Wang, J.D. Turner, B.K. Tsang, Changes in Tissue-Type Plasminogen Activator-Like and Plasminogen Activator Inhibitor Activities in Granulosa and Theca Layers during Ovarian Follicle Development in the Domestic Hen1, Biol. Reprod. 42 (1990) 747–754. doi:10.1095/biolreprod42.5.747.
[44] S. Petersen, A. Fahr, H. Bunjes, Flow cytometry as a new approach to investigate drug transfer between lipid particles, Mol. Pharm. 7 (2010) 350–363. doi:10.1021/mp900130s.
[45] V. Wintgens, C. Lorthioir, P. Dubot, B. Sébille, C. Amiel, Cyclodextrin/dextran based hydrogels prepared by cross-linking with sodium trimetaphosphate, Carbohydr. Polym. 132 (2015) 80–88. doi:10.1016/j.carbpol.2015.06.038.
[46] L. Arnfast, C.G. Madsen, L. Jorgensen, S. Baldursdottir, Design and processing of nanogels as delivery systems for peptides and proteins, Ther. Deliv. 5 (2014) 691–708. doi:10.4155/tde.14.38.
[47] Z.M. Ruggeri, Platelets in atherothrombosis, Nat. Med. 8 (2002) 1227–1234. doi:10.4065/81.1.59.
[48] T.J. Merkel, K. Chen, S.W. Jones, A.A. Pandya, S. Tian, M.E. Napier, W.E. Zamboni, J.M. Desimone, The effect of particle size on the biodistribution of low-modulus hydrogel PRINT particles, J. Control. Release. 162 (2012) 37–44. doi:10.1016/j.jconrel.2012.06.009.
[49] C. Orset, B. Haelewyn, S.M. Allan, S. Ansar, F. Campos, T.H. Cho, A. Durand, M. El Amki, M. Fatar, I. Garcia-Yébenes, M. Gauberti, S. Grudzenski, I. Lizasoain, E. Lo, R. Macrez, I. Margaill, S. Maysami, S. Meairs, N. Nighoghossian, J. Orbe, J.A. Paramo, J.J. Parienti, N.J. Rothwell, M. Rubio, C. Waeber, A.R. Young, E. Touzé, D. Vivien, Efficacy of Alteplase in a Mouse Model of Acute Ischemic Stroke: A Retrospective Pooled Analysis, Stroke. 47 (2016) 1312–1318. doi:10.1161/STROKEAHA.116.012238.
[50] S.M. De Lizarrondo, C. Gakuba, B.A. Herbig, Y. Repessé, C. Ali, C. V. Denis, P.J. Lenting, E. Touzé, S.L. Diamond, D. Vivien, M. Gauberti, Potent thrombolytic effect of N-acetylcysteine on arterial thrombi, Circulation. 136 (2017) 646–660. doi:10.1161/CIRCULATIONAHA.117.027290.
[51] H.R. Lijnen, B. Van Hoef, V. Beelen, D. Collen, Characterization of the Murine Plasma Fibrinolytic System, Eur. J. Biochem. 224 (1994) 863–871. doi:10.1111/j.1432-1033.1994.00863.x.
[52] R. Brouns, P.P. De Deyn, The complexity of neurobiological processes in acute ischemic stroke, Clin. Neurol. Neurosurg. 111 (2009) 483–495. doi:10.1016/j.clineuro.2009.04.001.
[53] A. Zenych, L. Fournier, C. Chauvierre, Nanomedicine progress in thrombolytic therapy, Biomaterials. 258 (2020) 120297. doi:10.1016/j.biomaterials.2020.120297.
[54] K.S. Masters, D.N. Shah, L.A. Leinwand, K.S. Anseth, Crosslinked hyaluronan scaffolds as a biologically active carrier for valvular interstitial cells, Biomaterials. 26 (2005) 2517–2525. doi:10.1016/j.biomaterials.2004.07.018.
[55] C.I. Jones, D.A. Payne, P.D. Hayes, A.R. Naylor, P.R.F. Bell, M.M. Thompson, A.H. Goodall, The antithrombotic effect of dextran-40 in man is due to enhanced fibrinolysis in vivo, J. Vasc. Surg. 48 (2008) 715–722. doi:10.1016/j.jvs.2008.04.008.

[56] E.M. Balboa, E. Conde, A. Moure, E. Falqué, H. Domínguez, In vitro antioxidant properties of crude extracts and compounds from brown algae, Food Chem. 138 (2013) 1764–1785. doi:10.1016/j.foodchem.2012.11.026.
[57] Y. Choi, S.K. Min, R. Usoltseva, A. Silchenko, T. Zvyagintseva, S. Ermakova, J.K. Kim, Thrombolytic fucoidans inhibit the tPA-PAI1 complex, indicating activation of plasma tissue-type plasminogen activator is a mechanism of fucoidan-mediated thrombolysis in a mouse thrombosis model, Thromb. Res. 161 (2018) 22–25. doi:10.1016/j.thromres.2017.11.015.
[58] K. Knop, R. Hoogenboom, D. Fischer, U.S. Schubert, Poly(ethylene glycol) in drug delivery: Pros and cons as well as potential alternatives, Angew. Chemie - Int. Ed. 49 (2010) 6288–6308. doi:10.1002/anie.200902672.
[59] M. Di Marco, K.A. Razak, A.A. Aziz, C. Devaux, E. Borghi, L. Levy, C. Sadun, Overview of the main methods used to combine proteins with nanosystems : absorption, bioconjugation, and encapsulation, Int. J. Nanomedicine. 5 (2010) 37–49.
[60] R.P. Friedrich, J. Zaloga, E. Schreiber, I.Y. Tóth, E. Tombácz, S. Lyer, C. Alexiou, Tissue Plasminogen Activator Binding to Superparamagnetic Iron Oxide Nanoparticle-Covalent Versus Adsorptive Approach, Nanoscale Res. Lett. 11 (2016) 1–11. doi:10.1186/s11671-016-1521-7.
[61] C.L. Pawlowski, W. Li, M. Sun, K. Ravichandran, D. Hickman, C. Kos, G. Kaur, A. Sen Gupta, Platelet microparticle-inspired clot-responsive nanomedicine for targeted fibrinolysis, Biomaterials. 128 (2017) 94–108. doi:10.1016/j.biomaterials.2017.03.012.
[62] J. Xu, Y. Zhang, J. Xu, G. Liu, C. Di, X. Zhao, X. Li, Y. Li, N. Pang, C. Yang, Y. Li, B. Li, Z. Lu, M. Wang, K. Dai, R. Yan, S. Li, G. Nie, Engineered Nanoplatelets for Targeted Delivery of Plasminogen Activators to Reverse Thrombus in Multiple Mouse Thrombosis Models, Adv. Mater. 1905145 (2019) 1–14. doi:10.1002/adma.201905145.
[63] J. Hu, S. Huang, L. Zhu, W. Huang, Y. Zhao, K. Jin, Q. Zhuge, Tissue Plasminogen Activator-Porous Magnetic Microrods for Targeted Thrombolytic Therapy after Ischemic Stroke, ACS Appl. Mater. Interfaces. 10 (2018) 32988–32997. doi:10.1021/acsami.8b09423.
[64] L. Huang, J. Wang, S. Huang, F. Siaw-Debrah, M. Nyanzu, Q. Zhuge, Polyacrylic acid-coated nanoparticles loaded with recombinant tissue plasminogen activator for the treatment of mice with ischemic stroke, Biochem. Biophys. Res. Commun. 516 (2019) 565–570. doi:10.1016/j.bbrc.2019.06.079.
[65] T. Mei, A. Kim, L.B. Vong, A. Marushima, S. Puentes, Y. Matsumaru, A. Matsumura, Y. Nagasaki, Encapsulation of tissue plasminogen activator in pH-sensitive self-assembled antioxidant nanoparticles for ischemic stroke treatment-Synergistic effect of thrombolysis and antioxidant, Biomaterials. 215 (2019) 1–12. doi:10.1016/j.biomaterials.2019.05.020.
[66] H. Kim, J.H. Ahn, M. Song, D.W. Kim, T.K. Lee, J.C. Lee, Y.M. Kim, J.D. Kim, J.H. Cho, I.K. Hwang, B.C. Yan, M.H. Won, J.H. Park, Pretreated fucoidan confers neuroprotection against transient global cerebral ischemic injury in the gerbil hippocampal CA1 area via reducing of glial cell activation and oxidative stress, Biomed. Pharmacother. 109 (2019) 1718–1727. doi:10.1016/j.biopha.2018.11.015.
[67] D. Vivien, M. Gauberti, A. Montagne, G. Defer, E. Touzé, Impact of tissue plasminogen activator on the neurovascular unit: From clinical data to experimental evidence, J. Cereb. Blood Flow Metab. 31 (2011) 2119–2134. doi:10.1038/jcbfm.2011.127.
[68] J.P.A. Ioannidis, B.Y.S. Kim, A. Trounson, How to design preclinical studies in nanomedicine and cell therapy to maximize the prospects of clinical translation, Nat. Biomed. Eng. 2 (2018) 797–809. doi:10.1038/s41551-018-0314-y.
[69] S. Yokoyama, H. Ikeda, N. Haramaki, H. Yasukawa, T. Murohara, T. Imaizumi, Platelet

P-selectin plays an important role in arterial thrombogenesis by forming large stable platelet-leukocyte aggregates, J. Am. Coll. Cardiol. 45 (2005) 1280–1286. doi:10.1016/j.jacc.2004.12.071.

[70] S.R. Barthel, J.D. Gavino, L. Descheny, C.J. Dimitroff, Targeting selectins and selectin ligands in inflammation and cancer, Expert Opin. Ther. Targets. 11 (2007) 1473–1491. doi:10.1517/14728222.11.11.1473.

[71] Y. Shamay, M. Elkabets, H. Li, J. Shah, S. Brook, F. Wang, K. Adler, E. Baut, M. Scaltriti, P. V Jena, E.E. Gardner, J.T. Poirier, C.M. Rudin, J. Baselga, A. Haimovitz-Friedman, D.A. Heller, P-selectin is a nanotherapeutic delivery target in the tumor microenvironment, Sci. Transl. Med. 8 (2016) 345ra87. doi:10.1126/scitranslmed.aaf7374.

[72] J.M. Lee, Z.-U. Shin, G.T. Mavlonov, I.Y. Abdurakhmonov, T.-H. Yi, Solid-Phase Colorimetric Method for the Quantification of Fucoidan, Appl. Biochem. Biotechnol. 168 (2012) 1019–1024. doi:10.1007/s12010-012-9837-y.

[73] C. Orset, R. Macrez, A.R. Young, D. Panthou, E. Angles-cano, E. Maubert, V. Agin, D. Vivien, Mouse Model of In Situ Thromboembolic Stroke and Reperfusion, Stroke. 38 (2007) 2771–2778. doi:10.1161/STROKEAHA.107.487520.

Supplementary Data

Fucoidan-Functionalized Polysaccharide Submicroparticles Loaded with Alteplase for Efficient Targeted Thrombolytic Therapy

Alina Zenych[1], Charlène Jacqmarcq[2,#], Rachida Aid[1,3,#], Louise Fournier[1], Laura M. Forero Ramirez[1], Thomas Bonnard[2], Denis Vivien[2,4,#], Didier Letourneur[1,#], and Cédric Chauvierre[1,*]

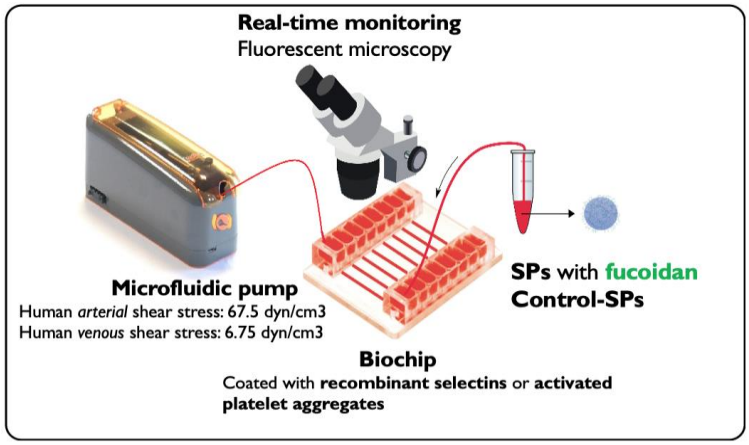

Figure S1. Schematic illustration of the *in vitro* targeting assay.

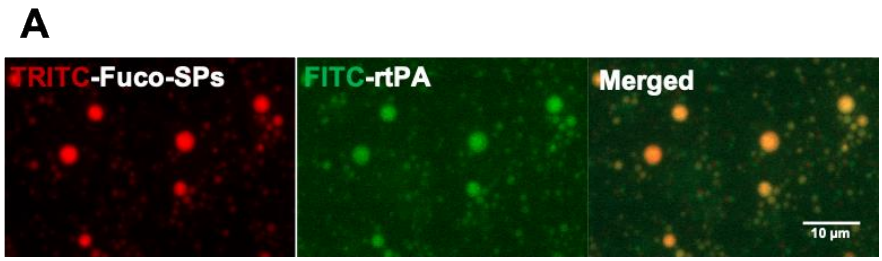

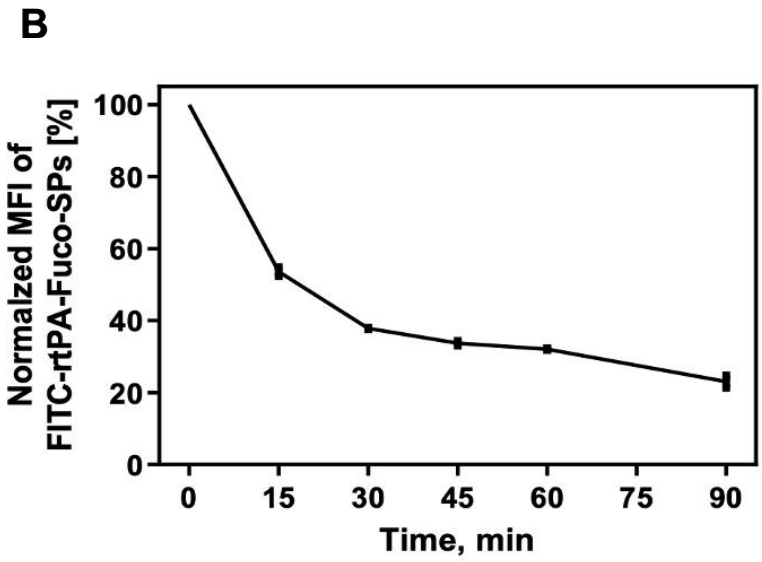

Figure S2. Loading and release of rtPA from Fuco-SPs. A. FITC-rtPA loading onto the TRITC-Fuco-SPs visualized by confocal microscopy. **B.** *In vitro* rtPA release from rtPA-encapsulated Fuco-SPs by flow cytometry.

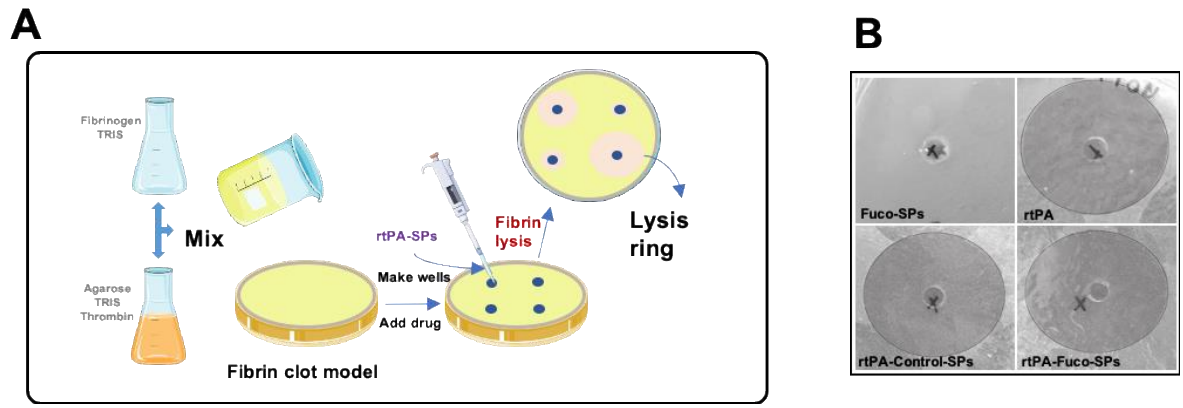

Figure S3. Fibrinolytic activity of the rtPA-loaded SPs *in vitro*. A. Schematic illustration of the *in vitro* fibrinolytic test. **B.** Lysed circles as the fibrinolytic potential of the SPs *in vitro* by a fibrin-plate agarose assay at the equal concentration of the rtPA.

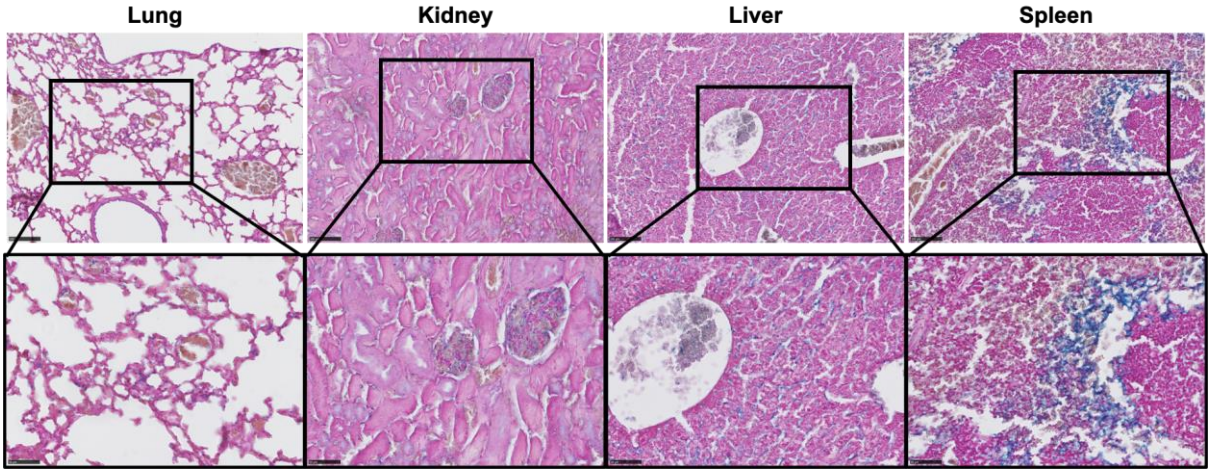

Figure S4. Histological analysis of Fuco-SPs in four organs of excretion. The cytoplasm appears pale pink, nuclei are red, and the Fuco-SPs are stained blue. Few particles were detected in the lungs, kidneys, and liver, whereas they were mainly accumulated in the spleen. The scale bar in the upper row = 100 μm, in the lower row (magnified image) = 50 μm.

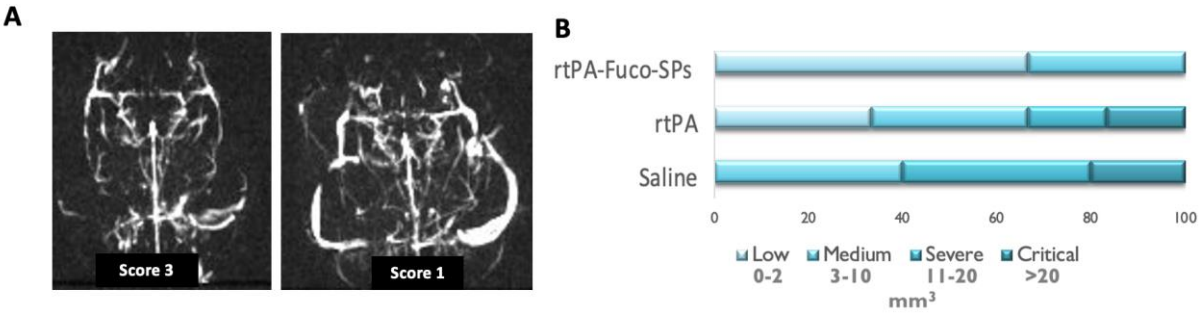

Figure S5. Therapeutic efficacy of the rtPA-Fuco-SPs *in vivo*. A. Merged image of the MRA scores (Score 3: full recanalization, score 1: low perfusion). **B.** Distribution of the cases by the infarct zone sizes by MRI 24 h post-stroke.

Video S1. Cerebral blood flow reperfusion monitored by the laser speckle contrast imaging during the 40-min treatment regimen with saline (**A**), rtPA (**B**), and rtPA-Fuco-SPs (**C**) in the ROI of ipsilateral (2) and contralateral (1) hemispheres.

Table S1. The synthesis parameters for the polysaccharide SPs.

Synthesis method	Polysaccharide [c], mg/ml	STMP, [c], mg/ml	NaOH [c], M	Phase ratio, (Aq/ Org/)	Surfactant	Homogenization	Crosslinking
W/O emulsion / crosslinking	300	56.11	1.15	4% w/v	PGPR, 6%	30,000 rpm, 4 min, 4 °C	20 min, 50 ° C

Abbreviation: W/O, water-in-oil; Aq, aqueous; Org organic.

Movie S1A

Click here to access/download

Movie/Animation

Movie S1A - Saline.avi

Movie S1B

Click here to access/download

Movie/Animation

Movie S1B - rtPA .avi

Movie S1C

Click here to access/download

Movie/Animation

Movie S1C - rtPA-Fuco SPs.avi